EUROPEAN ORGANISATION FOR NUCLEAR RESEARCH (CERN)

Submitted to: JHEP

CERN-EP-2024-246
30th September 2024

arXiv:2409.18762v1 [hep-ex] 27 Sep 2024

Search for supersymmetry using vector boson fusion signatures and missing transverse momentum in pp collisions at $\sqrt{s} = 13$ TeV with the ATLAS detector

The ATLAS Collaboration

This paper presents a search for supersymmetric particles in models with highly compressed mass spectra, in events consistent with being produced through vector boson fusion. The search uses 140 fb^{-1} of proton–proton collision data at $\sqrt{s}$ = 13 TeV collected by the ATLAS experiment at the Large Hadron Collider. Events containing at least two jets with a large gap in pseudorapidity, large missing transverse momentum, and no reconstructed leptons are selected. A boosted decision tree is used to separate events consistent with the production of supersymmetric particles from those due to Standard Model backgrounds. The data are found to be consistent with Standard Model predictions. The results are interpreted using simplified models of R-parity-conserving supersymmetry in which the lightest supersymmetric partner is a bino-like neutralino with a mass similar to that of the lightest chargino and second-to-lightest neutralino, both of which are wino-like. Lower limits at 95% confidence level on the masses of next-to-lightest supersymmetric partners in this simplified model are established at 117 GeV when the lightest supersymmetric partners are within 1 GeV in mass.

© 2024 CERN for the benefit of the ATLAS Collaboration.
Reproduction of this article or parts of it is allowed as specified in the CC-BY-4.0 license.

Contents

1 Introduction 2

2 ATLAS detector 4

3 Data and simulated event samples 5

4 Event reconstruction 7

5 Event selection and analysis strategy 8

6 Background estimation 9

7 Systematic uncertainties 12

8 Results 14

9 Conclusion 19

1 Introduction

Weak interactions at hadron colliders offer both challenges and opportunities in searches for physics beyond the Standard Model (SM). Despite their small cross-sections and low-momentum final states when compared with strong interactions, the signatures of weak interactions can enable discoveries of rare processes, such as: single-boson production through vector boson fusion (VBF) [1–3]; diboson production through vector-boson scattering (VBS) [4–13]; and triboson production [14–21]. Pure-electroweak processes, such as VBS and VBF, have emerged as powerful new tools, used most notably in studies of the Higgs boson (see e.g. Ref. [22]). The extremely low production cross-sections of such processes, typically smaller than a picobarn for pair-production of weak-scale particles, are mitigated by final states with a unique signature of two high-momentum jets with large separation in rapidity. The large amount of collision data available from the CERN Large Hadron Collider (LHC) increasingly enables the use of such weak production modes, and their distinctive features, in searches for physics beyond the Standard Model.

One extension of the Standard Model that has so far eluded discovery at the LHC is Supersymmetry (SUSY) [23–28], which predicts new particles that have identical quantum numbers to their SM partners with the exception of spin, with SM fermions having bosonic partners and SM bosons having fermionic partners. Problems such as those related to naturalness [29, 30] and the nature of dark matter motivate extensions of the SM like SUSY that are intimately connected with electroweak symmetry breaking.

SUSY models that address the naturalness problem often have some SUSY partners with masses near the electroweak scale. Models with weakly interacting massive particle (WIMP) dark matter candidates can avoid overabundance of dark matter through co-annihilation mechanisms, which arise in SUSY models with compressed mass spectra that feature SUSY partners with nearly degenerate masses [31–33]. SUSY scenarios featuring compressed mass spectra can result in collisions at the LHC in which SUSY particles are produced, but their SM decay products have such low momenta that they avoid detection. In R-parity conserving SUSY models [34] the lightest supersymmetric particles (LSPs) are stable and often carry

no electric charge, presenting viable dark matter candidates [35, 36]. Since they do not interact with the detector, such LSPs are only indirectly observed through the momentum imbalance in the transverse plane left by their escape. Detection of a SUSY signal in such events is challenged by large backgrounds and, in models where the lightest SUSY partners are the SUSY counterparts of SM electroweak bosons, by low signal cross-sections. One strategy for improving the sensitivity of searches for low-mass electroweak SUSY is to require additional hadronic activity in the event, which has the dual effect of providing a significant Lorentz boost to the SUSY particles and adding another visible physics object to the final state. The resulting signature provides better separation of the SUSY signal from SM backgrounds.

Following this strategy, this paper presents a search for compressed, electroweak SUSY in events with large missing transverse momentum, two or more jets rendering a VBF topology, and no reconstructed electrons or muons. The search is optimised for SUSY models with LSP masses within 2 GeV of the next-to-lightest SUSY partner (NLSP) mass, where the LSP is taken to be a bino-like neutralino ($\widetilde{\chi}_1^0$), and the mass-degenerate NLSPs include a neutralino ($\widetilde{\chi}_2^0$) and a pair of charginos ($\widetilde{\chi}_1^\pm$), all of which are wino-like. A broad collection of signature-based searches was studied in the context of the phenomenological minimal supersymmetric extension of the SM (pMSSM) in Ref. [37], and the region with $\Delta m(\widetilde{\chi}_2^0, \widetilde{\chi}_1^0) < 2$ GeV was found to be poorly constrained, motivating a focus on this region of SUSY parameter space. The $\widetilde{\chi}_2^0$, $\widetilde{\chi}_1^\pm$and $\widetilde{\chi}_1^0$ states are collectively referred to as electroweakinos in the following. The decays of unstable electroweakinos in this simplified model are assumed to proceed through emission of off-shell W or Z bosons, which then decay into fermions. At such small mass splittings the final decay products of the $\widetilde{\chi}_2^0$ and $\widetilde{\chi}_1^\pm$ have sufficiently low momenta that they are not reconstructed in the detector, motivating the zero-lepton signature. The two jets can arise from either QCD couplings or pure-electroweak couplings. In the pure-electroweak case, the SUSY particles can be produced through a VBF process, illustrated in Figure 1(a). Other diagrams with QCD couplings, such as Figure 1(b), result in the same final state and interfere with the VBF process. The contributions of the VBF diagrams motivate searches in events characterised by large separation between jets and large dijet invariant mass.

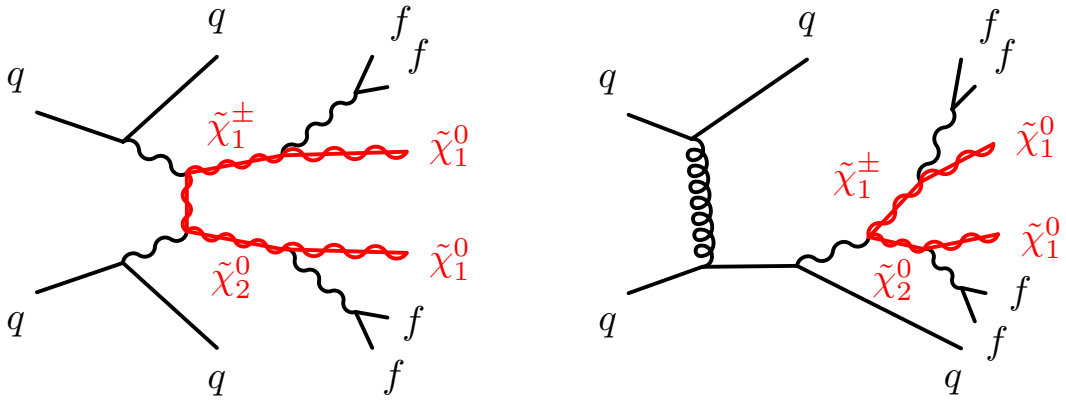

Figure 1: Diagrams illustrating both (a) pure-electroweak and (b) mixed electroweak-QCD production of electroweakino pairs in association with two jets.

The use of the VBF signature as a way to probe SUSY models has been proposed several times [38–41]. This approach was explored experimentally by the CMS experiment in proton-proton (pp) collision data at $\sqrt{s}$ = 8 TeV in Ref. [42], and at $\sqrt{s}$ = 13 TeV in Ref. [43]. ATLAS studied the VBF final state in pp collision data at $\sqrt{s}$ = 13 TeV in a two-lepton search for SUSY in Ref. [44], and CMS presented SUSY

searches in one- and zero-lepton topologies in Ref. [43]. Similar final states have also been used to constrain the branching ratio of Higgs bosons to invisible final states [45, 46]. The kinematic selections applied in the latter analyses were optimised for the production of a single SM Higgs boson, rendering them less sensitive to the SUSY scenarios considered in this paper in which fermionic electroweakinos are pair-produced with an overall mass of roughly twice the mass of the SM Higgs boson. ATLAS has also performed a differential cross-section measurement of dijet kinematics in events with missing transverse momentum in VBF phase space [47], which observed good modelling of most kinematic distributions except the dijet invariant mass, partially motivating dedicated searches for non-SM contributions in this signature.

2 ATLAS detector

The ATLAS detector [48] at the LHC covers nearly the entire solid angle around the collision point.[1] It consists of an inner tracking detector surrounded by a thin superconducting solenoid, electromagnetic and hadronic calorimeters, and a muon spectrometer incorporating three large superconducting air-core toroidal magnets.

The inner-detector system (ID) is immersed in a 2 T axial magnetic field and provides charged-particle tracking in the range $|\eta| < 2.5$. The high-granularity silicon pixel detector covers the vertex region and typically provides four measurements per track, the first hit generally being in the insertable B-layer (IBL) installed before Run 2 [49, 50]. It is followed by the SemiConductor Tracker (SCT), which usually provides eight measurements per track. These silicon detectors are complemented by the transition radiation tracker (TRT), which enables radially extended track reconstruction up to $|\eta| = 2.0$. The TRT also provides electron identification information based on the fraction of hits (typically 30 in total) above a higher energy-deposit threshold corresponding to transition radiation.

The calorimeter system covers the pseudorapidity range $|\eta| < 4.9$. Within the region $|\eta| < 3.2$, electromagnetic calorimetry is provided by barrel and endcap high-granularity lead/liquid-argon (LAr) calorimeters, with an additional thin LAr presampler covering $|\eta| < 1.8$ to correct for energy loss in material upstream of the calorimeters. Hadronic calorimetry is provided by the steel/scintillator-tile calorimeter, segmented into three barrel structures within $|\eta| < 1.7$, and two copper/LAr hadronic endcap calorimeters. The solid angle coverage is completed with forward copper/LAr and tungsten/LAr calorimeter modules optimised for electromagnetic and hadronic energy measurements respectively.

The muon spectrometer (MS) comprises separate trigger and high-precision tracking chambers measuring the deflection of muons in a magnetic field generated by the superconducting air-core toroidal magnets. The field integral of the toroids ranges between 2.0 and 6.0 T m across most of the detector. Three layers of precision chambers, each consisting of layers of monitored drift tubes, cover the region $|\eta| < 2.7$, complemented by cathode-strip chambers in the forward region, where the background is highest. The muon trigger system covers the range $|\eta| < 2.4$ with resistive-plate chambers in the barrel, and thin-gap chambers in the endcap regions.

[1] ATLAS uses a right-handed coordinate system with its origin at the nominal interaction point (IP) in the centre of the detector and the z-axis along the beam pipe. The x-axis points from the IP to the centre of the LHC ring, and the y-axis points upwards. Polar coordinates (r, ϕ) are used in the transverse plane, ϕ being the azimuthal angle around the z-axis. The pseudorapidity is defined in terms of the polar angle θ as $\eta = -\ln\tan(\theta/2)$ and is equal to the rapidity $y = \frac{1}{2}\ln\left(\frac{E+p_z c}{E-p_z c}\right)$ in the relativistic limit. Angular distance is measured in units of $\Delta R \equiv \sqrt{(\Delta y)^2 + (\Delta\phi)^2}$.

The luminosity is measured mainly by the LUCID–2 [51] detector that records Cherenkov light produced in the quartz windows of photomultipliers located close to the beampipe.

Events are selected by the first-level trigger system implemented in custom hardware, followed by selections made by algorithms implemented in software in the high-level trigger [52]. The first-level trigger accepts events from the 40 MHz bunch crossings at a rate below 100 kHz, which the high-level trigger further reduces in order to record complete events to disk at about 1 kHz.

A software suite [53] is used in data simulation, in the reconstruction and analysis of real and simulated data, in detector operations, and in the trigger and data acquisition systems of the experiment.

3 Data and simulated event samples

Data events were selected with a missing transverse momentum ($\mathbf{p}_{\mathrm{T}}^{\mathrm{miss}}$) trigger [54], employing varied trigger thresholds depending on the data-taking periods. The trigger is > 95% efficient in all data-taking periods for events where the offline magnitude of $\mathbf{p}_{\mathrm{T}}^{\mathrm{miss}}$, conventionally denoted by $E_{\mathrm{T}}^{\mathrm{miss}}$, is above 200 GeV. In addition, events selected by single-electron (muon) triggers [55, 56] are considered to collect a sample of events to constrain the dominant SM backgrounds with online lepton transverse momentum (p_{T}) thresholds starting from 24–26 (20–24) GeV dependent on the period of data taking. The data sample used corresponds to 140 fb^{-1} of $\sqrt{s}$ = 13 TeV pp collision data, where the uncertainty in the integrated luminosity is 0.83% [57]. The average number of interactions per bunch-crossing was 33.7.

Samples of Monte Carlo (MC) simulated events are used to estimate the signal yields, and to estimate the background from SM processes with significant $E_{\mathrm{T}}^{\mathrm{miss}}$ from invisible particles such as neutrinos. MC samples are also used to derive systematic uncertainties in the signal and background predictions.

The SUSY signal is modelled using MadGraph5_aMC@NLO 2.7.3 [58] with the NNPDF2.3LO [59] parton distribution function (PDF) set. Pythia 8.244 [60] is used to model the parton shower, hadronisation, and underlying event, using the A14 set of tuned parameters [61].

Simulated signal samples consist of wino-like $\widetilde{\chi}_2^0\widetilde{\chi}_1^\pm$, $\widetilde{\chi}_1^\pm\widetilde{\chi}_1^\mp$, $\widetilde{\chi}_2^0\widetilde{\chi}_2^0$, and $\widetilde{\chi}_1^\pm\widetilde{\chi}_1^\pm$ production in association with exactly two additional partons in the final state.[2] The parton-level jets are required to have $p_{\mathrm{T}} > 30$ GeV and to be separated by at least 2.5 units in pseudorapidity. MadSpin [62] is used to decay the electroweakinos into a $\widetilde{\chi}_1^0$ and a pair of SM fermions. The generated samples cover scenarios of $\widetilde{\chi}_2^0/\widetilde{\chi}_1^\pm$ masses between 75–175 GeV and mass splittings between the NLSPs and LSP of 0.2–5 GeV. While the signal kinematics do not depend strongly on the electroweakino mass in this regime, samples with larger mass splittings feature more energetic leptons in the decay chain rendering such signals less efficient to the zero-lepton requirement of the analysis. Samples are normalised to leading-order (LO) cross-sections from MadGraph5_aMC@NLO assuming pure wino-like states. The total signal cross-section including all production modes ranges from approximately 1.6 pb to 0.06 pb for $\widetilde{\chi}_2^0/\widetilde{\chi}_1^\pm$ masses between 75 GeV and 175 GeV. Some kinematics of the SM decay products are sensitive to the relative sign of the signed mass eigenvalues $m(\widetilde{\chi}_2^0)$ and $m(\widetilde{\chi}_1^0)$; in this analysis, the product $m(\widetilde{\chi}_2^0) \times m(\widetilde{\chi}_1^0)$ is assumed to be positive.[3]

[2] The $\widetilde{\chi}_2^0\widetilde{\chi}_2^0$, $\widetilde{\chi}_1^+\widetilde{\chi}_1^+$ and $\widetilde{\chi}_1^-\widetilde{\chi}_1^-$ productions feature only pure-electroweak diagrams while the others production modes occur also via mixed electroweak-QCD couplings.

[3] The mixing matrix used to diagonalise the neutral electroweakino states can be complex but is forced to be a real matrix in the SLHA2 format [63] at the cost of introducing negative mass eigenstates. The sign will affect the couplings and thus the distributions in the decay under consideration. For additional discussion of this, see Ref. [64] and Appendix A in Ref. [65].

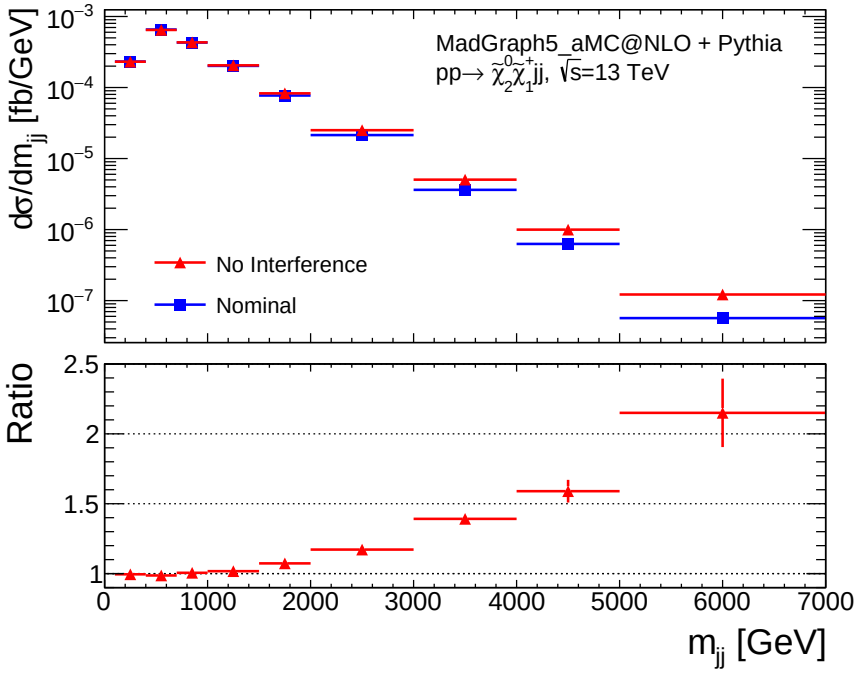

Figure 2: Comparison of different process definitions for $\widetilde{\chi}_2^0\widetilde{\chi}_1^+$ production in association with two jets, made at particle level using the anti-k_t algorithm with a radius parameter of $R = 0.4$. The 'Nominal' sample is generated according to the details in Section 3. The 'No Interference' sample generates pure-electroweak processes separately from processes with mixed electroweak-QCD couplings. Events are selected by requiring two jets with $p_{\mathrm{T}} > 30$ GeV and $|\eta| < 5.0$, and oppositely signed pseudorapidities.

Production of two electroweakinos in association with two jets can proceed through either VBF-like diagrams with a t-channel process, such as those shown in Figure 1(a), or s-channel diagrams such as Figure 1(b). The s-channel diagrams can also be either pure-electroweak, in which the boson exchanged by incoming partons is a photon, W boson, or Z boson, or have both electroweak and QCD couplings, in which case the exchanged boson is a gluon. All such diagrams have identical initial and final states, and all must therefore be included to ensure gauge-invariant predictions. The interference between these diagrams affects the total cross-section and the kinematics in phase space traditionally targeted by VBF searches, such as large dijet invariant mass (m_{jj}) and large pseudorapidity separation between jets ($\Delta\eta_{\mathrm{jj}}$). The effect of the interference in these SUSY models is illustrated in Figure 2, where the impact on the inclusive cross-section is modest, but can be a factor of two or more for $m_{\mathrm{jj}} > 5$ TeV.

The SM background processes are estimated from a combination of MC simulation samples and data-driven approaches. The most important backgrounds, from SM $Z \to \nu\nu$ and $W \to \ell\nu$ events (where the lepton is not reconstructed), are modelled with Sherpa 2.2.11 [66] using the NNPDF3.0NNLO PDF set [67]. For strong production of V + jets ($V = W, Z, \gamma^*$), where a QCD coupling facilitates the production of the additional jets, processes with up to two coloured partons are modelled at next-to-leading-order (NLO) in the strong coupling, while processes with up to five additional partons are modelled at LO accuracy. Electroweak production of V + jets is modelled separately using the same generator, in which processes with up to two partons are modelled at LO accuracy.

Subdominant backgrounds include SM diboson production, events with one or more top quarks, and

triboson production. Diboson production with either fully leptonic or semileptonic decays of the bosons is modelled with Sherpa 2.2.1 or 2.2.2 (depending on the process) at NLO accuracy for up to one additional parton, and at LO accuracy for up to three additional partons. Electroweak diboson production with fully leptonic decays is modelled with Sherpa 2.2.12 at LO accuracy with up to one additional parton. The $t\bar{t}$ and single top-quark processes are generated at NLO with Powheg Box v2 [68–71] for the matrix element, using the NNPDF3.0NLO PDF set [67], and Pythia 8.230 for the parton shower. The diagram removal scheme [72] is used to account for interference between $t\bar{t}$ and Wt. Triboson production was modelled with Sherpa 2.2.2 at NLO for inclusive processes, and at LO for up to two additional parton emissions, using the NNPDF3.0NNLO PDF set.

The effect of multiple interactions in the same and neighbouring bunch crossings (pile-up) is modelled by overlaying the simulated hard-scattering event with inelastic pp collisions generated with Pythia 8.186 [73] using the NNPDF2.3LO PDF set and the A3 set of tuned parameters [74]. The MC events are weighted to reproduce the distribution of the average number of interactions per bunch crossing observed in the data.

Background and signal samples make use of EvtGen 1.6.0 and 1.2.0 [75] to model the decay of b- and c-hadrons, with the exception of the background samples modelled with Sherpa, which performs these decays internally. All MC simulated samples are processed through the ATLAS simulation framework [76] in Geant4 [77], except the signal samples, which are processed with a fast simulation which relies on a parameterisation of the calorimeter response [78].

4 Event reconstruction

Each event is required to have a primary vertex built from at least two associated tracks with $p_{\mathrm{T}} > 0.5$ GeV. The primary vertex with the highest sum of squared transverse momenta $\sum p_{\mathrm{T}}^2$ of associated tracks [79] is selected as the hard-scatter vertex of interest in each event. As described below, reconstructed jets and leptons are categorised according to 'baseline' and 'signal' criteria, where the latter category includes tighter requirements on the quality of the reconstructed object.

Hadronic jets are reconstructed using the anti-k_t algorithm [80, 81] with a radius parameter of $R = 0.4$ using particle-flow objects [82] calibrated at the electromagnetic (EM) scale. The jet energy scale and resolution are calibrated using simulations with in situ corrections obtained from data [83]. Baseline jets, used for removing overlaps between different types of physics objects, are required to satisfy $p_{\mathrm{T}} > 20$ GeV and $|\eta| < 4.5$. Signal jets, which are a subset of baseline jets and are used for event selection and categorisation, must satisfy stricter requirements that suppress contributions from additional pp collisions in the same or nearby bunch crossings. All signal jets are required to have $p_{\mathrm{T}} > 30$ GeV. Central signal jets with $|\eta| < 2.4$ must additionally satisfy the *Medium* working point of the jet vertex tagger [84] if they have $p_{\mathrm{T}} < 60$ GeV. Signal jets with $2.4 < |\eta| < 4.5$ must satisfy the *Loose* working point of the forward jet vertex tagger [85] if they have $p_{\mathrm{T}} < 120$ GeV. Jets within $|\eta| < 2.5$ that satisfy the 85% efficiency working point of the DL1r algorithm [86] are identified as containing b-hadrons and are referred to as b-tagged jets.

Baseline electrons are reconstructed using ID tracks matched to energy clusters in the EM calorimeter. These satisfy $p_{\mathrm{T}} > 4.5$ GeV and $|\eta| < 2.47$ with a *LooseAndBLayerLLH* identification [87]. The longitudinal impact parameter z_0 of baseline electron tracks is required to satisfy $|z_0 \sin\theta| < 0.5$ mm. Signal electrons must also satisfy the *Tight* likelihood-based identification criteria as well as the *Loose_VarRad* isolation requirements [88], and have a transverse impact parameter d_0 with uncertainty $\sigma(d_0)$ satisfying $|d_0/\sigma(d_0)| < 5$.

Baseline muons are reconstructed by combining tracks from the ID and the muon spectrometer subsystems. The *Loose* identification criteria [89] are applied. Baseline muons are required to have $p_{\mathrm{T}} > 3$ GeV and $|\eta| < 2.7$, and satisfy $|z_0 \sin\theta| < 0.5$ mm. Signal muons must also have $|\eta| < 2.5$, satisfy the *Medium* identification requirements and *Loose_VarRad* isolation criteria, and have impact parameter significance $|d_0/\sigma(d_0)| < 3$.

To prevent the use of the same reconstructed detector signals in multiple objects, an overlap removal procedure is applied to the baseline leptons and jets in the following order. First, any electron sharing an ID track with a muon is removed. Next, jets are removed if they are within $\Delta R < 0.2$ from a remaining electron. After this, electrons are in turn rejected if they are within $0.4 < \Delta R < \min(0.4, 0.04 + 10\ \mathrm{GeV}/p_{\mathrm{T}}(e))$ of any remaining jet. Jets are removed if they are closer than $\Delta R < 0.4$ to a muon and the jet has fewer than three associated tracks with $p_{\mathrm{T}} > 500$ MeV. Finally, any muon within $0.4 < \Delta R < \min(0.4, 0.04 + 10\ \mathrm{GeV}/p_{\mathrm{T}}(\mu))$ of a jet are removed.

The missing transverse momentum is calculated as the negative vector sum of the transverse momenta of all baseline leptons and jets calibrated to their respective energy scales, and an additional soft term constructed from tracks originating from the hard-scatter vertex but not associated with any of the reconstructed objects [90].

5 Event selection and analysis strategy

Several cleaning criteria are applied to all events, including a requirement that the leading jet satisfy the *Tight* jet cleaning criterion to efficiently veto non-collision backgrounds [91].

All events used in the analysis are required to have zero b-tagged jets, and at least two jets with oppositely signed pseudorapidity. If multiple pairs of jets satisfying that requirement are present in the event, then the jet pair with the largest value of m_{jj} is chosen to represent the VBF tagging jets. The VBF tagging jet with higher p_{T} is labelled $\mathrm{j}_1^{\mathrm{VBF}}$, while the subleading jet is labelled $\mathrm{j}_2^{\mathrm{VBF}}$. Events satisfy the preselection criteria and are retained for further study if they contain a VBF pair that satisfies $m_{\mathrm{jj}} > 600$ GeV, $|\Delta\eta_{\mathrm{jj}}| > 3.0$, $p_{\mathrm{T}}\left(\mathrm{j}_1^{\mathrm{VBF}}\right) > 80$ GeV, and have all baseline jets sufficiently well-separated from the $\mathbf{p}_{\mathrm{T}}^{\mathrm{miss}}$ in ϕ to satisfy $\min\left(\Delta\phi\left(\mathbf{j}, \mathbf{p}_{\mathrm{T}}^{\mathrm{miss}}\right)\right) > 0.4$ in order to suppress the multijet background.

Events that enter the signal region (SR) are preselected events that first satisfy a set of additional requirements that enhance the sensitivity of the analysis to the SUSY signal. Specifically, events in the SR must contain zero signal electrons or muons, satisfy the inclusive-$E_{\mathrm{T}}^{\mathrm{miss}}$ trigger, and have $E_{\mathrm{T}}^{\mathrm{miss}} > 250$ GeV.

A boosted decision tree (BDT) is trained on the preselected signal and SM background MC events described in Section 3 to provide the final requirement used to select events for the SR. The LightGBM [92] framework is used to construct the BDT, which is trained to separate the SUSY signal from background events originating the SM processes described in Section 3, weighted according to their cross-section. Gradient boosting with the binary cross entropy as optimisation objective was used to train the BDT. The maximum number of trees in the BDT is restricted to 1500 where each tree has a maximum depth and number of leaves of five and eight, respectively. Only signal samples with $m(\widetilde{\chi}_2^0, \widetilde{\chi}_1^{\pm}) = 100$ GeV were supplied in the training to optimise the BDT performance for this mass regime. A k-fold cross-validation (with $k = 5$) approach is employed, with one fold used for validation, one fold used for testing, and the remaining folds used for training.

The list of input variables for the BDT consists of: $E_{\mathrm{T}}^{\mathrm{miss}}$; p_{T} of the two individual VBF-tagged jets; the p_{T} sum of the VBF-tagged jets as well as the same sum divided by $E_{\mathrm{T}}^{\mathrm{miss}}$; the separation in pseudorapidity $\Delta\eta_{\mathrm{jj}}$, and separation in polar angle $\Delta\phi_{\mathrm{jj}}$, of the two VBF-tagged jets; the separation in ϕ between the two VBF tagged jets and $\mathbf{p}_{\mathrm{T}}^{\mathrm{miss}}$, $\Delta\phi(\mathbf{j}, \mathbf{p}_{\mathrm{T}}^{\mathrm{miss}})$, as well as the absolute value of the difference $|\Delta\phi(\mathbf{j}_1^{\mathrm{VBF}}, \mathbf{p}_{\mathrm{T}}^{\mathrm{miss}}) - \Delta\phi(\mathbf{j}_2^{\mathrm{VBF}}, \mathbf{p}_{\mathrm{T}}^{\mathrm{miss}})|$; two transverse masses m_{T}, one for each of the VBF-tagged jets, as well as the sum of the two transverse masses, where the transverse mass is computed as $m_{\mathrm{T}}(\mathbf{j}, \mathbf{p}_{\mathrm{T}}^{\mathrm{miss}}) = \sqrt{2p_{\mathrm{T}}^{j}E_{\mathrm{T}}^{\mathrm{miss}}(1 - \cos(\Delta\phi(\mathbf{j}, \mathbf{p}_{\mathrm{T}}^{\mathrm{miss}})))}$; properties of the VBF jet system (m_{jj} and p_{T}); the weighted sum of m_{jj} and $E_{\mathrm{T}}^{\mathrm{miss}}$, where the weighted sum is calculated as m_{jj}/1430 GeV + $E_{\mathrm{T}}^{\mathrm{miss}}$/320 GeV with the 'normalisation' values in the denominators representing the average of m_{jj} and $E_{\mathrm{T}}^{\mathrm{miss}}$ of the SM background at preselection level, respectively; the minimum ϕ separation of any baseline jet with the $\mathbf{p}_{\mathrm{T}}^{\mathrm{miss}}$; and the m_{T} and separation in ϕ of the Υ- and Ξ-tagged jets with the $\mathbf{p}_{\mathrm{T}}^{\mathrm{miss}}$, where jet Υ minimises $\Delta\phi(\mathbf{j}, \mathbf{p}_{\mathrm{T}}^{\mathrm{miss}})$, and jet Ξ minimises $m_{\mathrm{T}}(\mathbf{j}, \mathbf{p}_{\mathrm{T}}^{\mathrm{miss}})$ using all baseline jets passing the overlap removal as candidates for Υ and Ξ.

The result of the BDT is a score assigned to each event, where scores close to unity are more consistent with signal processes, while scores close to zero are more similar to background processes. The most important input features were found to be $\Delta\eta_{\mathrm{jj}}$ and the p_{T} of the subleading jet. Only events with scores above 0.6 are kept in the SR; control and validation regions use events with BDT scores as low as 0.4, as described in Section 6. Depending the region, the BDT score distribution is either considered inclusively within some range, or binned in steps of 0.04, except the last bin, which covers scores from 0.88 to 1.0. This last bin shows the best sensitivity to the benchmark signals and is hence also used as single-bin SR to derive constraints on the number of events from generic physics processes beyond the SM as described in Section 8. After the training of the BDT, events in the SR are further split into two channels based on their jet multiplicity (N_{jets}): one channel containing events with exactly two jets (dubbed as '2j' in the following), and another containing events with three or more jets ('≥3j'). This split mildly increases the sensitivity but in particular takes into account the observed dependence of the normalisation and modelling uncertainties of the V + jets backgrounds as described below.

6 Background estimation

Predictions for SM background contributions to the SR are made using different strategies depending on the background process. The largest backgrounds arise from W and Z bosons produced in association with two or more jets, which are modelled using MC samples that are normalised in dedicated control regions (CRs). Backgrounds from processes that produce $E_{\mathrm{T}}^{\mathrm{miss}}$ through jet mismeasurement or instrumental effects (referred to here as multijet backgrounds) are modelled using a data-driven method. All other subdominant backgrounds listed in Section 3 are modelled using MC.

Monte Carlo predictions of Z + jets, where the Z boson decays into $\nu\bar{\nu}$, are normalised in CRs identical to the SRs except that they require the presence of two opposite-sign, same-flavour signal leptons with an invariant mass within 30 GeV of the Z-boson mass. The lepton momenta are added to the $\mathbf{p}_{\mathrm{T}}^{\mathrm{miss}}$ for the purposes of applying the $E_{\mathrm{T}}^{\mathrm{miss}}$ requirements in the SR and calculating the BDT inputs using this adjusted definition of $\mathbf{p}_{\mathrm{T}}^{\mathrm{miss}}$. This approach allows using $Z \to ee/\mu\mu$ events as proxy for the $Z \to \nu\bar{\nu}$ background present in the SR. Events in CR$-Z$ are collected using single-lepton triggers. To ensure stable trigger efficiencies the leptons in CR$-Z$ are required to be sufficiently energetic and lie within detector acceptance. Thus, the leading lepton is required to have a $p_{\mathrm{T}} > 27$ GeV and must be matched to the online trigger object. To efficiently veto mis-identified electrons, the energy deposits of each electron in the EM calorimeter must

Table 1: Summary of the selections defining the CRs, VRs and SRs. Each region is additionally split into 2j and ≥3j categories. The requirements of the preselection described in the text and on the number of baseline and signals leptons defined in Section 4 are also applied. The $E_{\mathrm{T}}^{\mathrm{miss}}/\sqrt{\Sigma E_{\mathrm{T}}}$ requirement for the W + jets regions is only applied to events with electrons, to enhance the fraction of W + jets in those regions.

Feature	CR−Z	VR−Z	CR−W	VR−W	VR−0L	Multi-bin SR	Single-bin SR
N_{leptons}	2		1		0		
$m_{\ell\ell}$	$\lvert m_{\ell\ell} - m_Z \rvert < 30$ GeV		–		–		
$E_{\mathrm{T}}^{\mathrm{miss}}/\sqrt{\Sigma E_{\mathrm{T}}}$	–		$E_{\mathrm{T}}^{\mathrm{miss}}/\sqrt{\Sigma E_{\mathrm{T}}} > 5\ \sqrt{\mathrm{GeV}}$		–		
BDT score	[0.50, 0.84)	[0.84, 1.0]	[0.50, 0.84)	[0.84, 1.0]	[0.4, 0.6)	[0.6, 1.0]	[0.88, 1.0]
BDT score bins	1	2	1	2	5	8	1

satisfy $|\eta| < 1.37$ or $1.52 < |\eta| < 2.47$ and the subleading electron must have $p_{\mathrm{T}} > 25$ GeV. Subleading muons must have $p_{\mathrm{T}} > 9$ GeV, with both muons satisfying $|\eta| < 2.5$.

The W + jets predictions are normalised in separate CRs that includes events with exactly one signal lepton. As with CR−Z, the lepton momentum is added to the $\mathbf{p}_{\mathrm{T}}^{\mathrm{miss}}$ before application of the remaining SR criteria and calculation of the BDT score. A combination of single-lepton triggers and the inclusive-$E_{\mathrm{T}}^{\mathrm{miss}}$ trigger are used to collect events in this CR. Due to larger rates of multijet processes in which a hadron (or one of its decay products) is misidentified as a lepton, additional kinematic requirements are imposed to enhance the fraction of W + jets in this region. This includes requiring leptons to satisfy $p_{\mathrm{T}} > 27$ GeV, and for electron events requiring $E_{\mathrm{T}}^{\mathrm{miss}}/\sqrt{\Sigma E_{\mathrm{T}}} > 5.0\ \sqrt{\mathrm{GeV}}$, where $\Sigma E_{\mathrm{T}} = p_{\mathrm{T}}(j_1) + p_{\mathrm{T}}(j_2) + p_{\mathrm{T}}(e)$, with $E_{\mathrm{T}}^{\mathrm{miss}}/\sqrt{\Sigma E_{\mathrm{T}}}$ used as an approximation of the $E_{\mathrm{T}}^{\mathrm{miss}}$ significance [93].

Events in CR−W and CR−Z are required to have BDT scores between 0.5 and 0.84, and are split into 2j and ≥3j channels in accordance with the SRs. This allows the normalisation of the W and Z backgrounds individually for each category, resulting in four normalisation factors in total. While the lower requirement on the BDT score ensures that the normalisation factors are derived in a phase space similar to the SRs, events with BDT scores between 0.84 and 1.0 are reserved for validation regions (VRs) used to check the extrapolation of the V + jets predictions into high-BDT regions, which provide the best sensitivity to SUSY signals in the SRs. Distributions of the BDT scores for CR−W and CR−Z in both the 2j and ≥3j channels are shown in Figure 3. In addition, a separate set of validation regions, called VR-0L, are constructed from SR events with BDT scores between 0.4 and 0.6 to validate the extrapolation of the V + jets normalisations derived in one- or two-lepton regions to the zero-lepton phase space. A summary of the selections employed to define the regions used in the analysis is presented in Table 1.

A small but non-negligible amount of SM background also originates from multijet processes in which the $E_{\mathrm{T}}^{\mathrm{miss}}$ originates from mismeasured jets. It would be computationally expensive to simulate this background with sufficient MC statistics in the high-$E_{\mathrm{T}}^{\mathrm{miss}}$ phase space considered in this search. Hence, multijet backgrounds are estimated via a semi data-driven approach using dedicated CRs enriched by multijet contributions utilising an 'ABCD'-like region layout where 'D' labels the phase space of the SR for which the multijet estimate is derived. The region CR-A is identical to the SR, except for a requirement that $\min\left(\Delta\phi\left(\mathbf{j}, \mathbf{p}_{\mathrm{T}}^{\mathrm{miss}}\right)\right) < 0.4$. Regions CR-B and CR-C are identical to CR-A and the SR, respectively, except that they require events to have $200 < E_{\mathrm{T}}^{\mathrm{miss}}/\mathrm{GeV} < 220$ and BDT scores above 0.4 to be orthogonal but still kinematically similar to the SR. The inclusive yield N_{SR} of multijet events in the SR, i.e. integrated over all SR bins, is then computed as

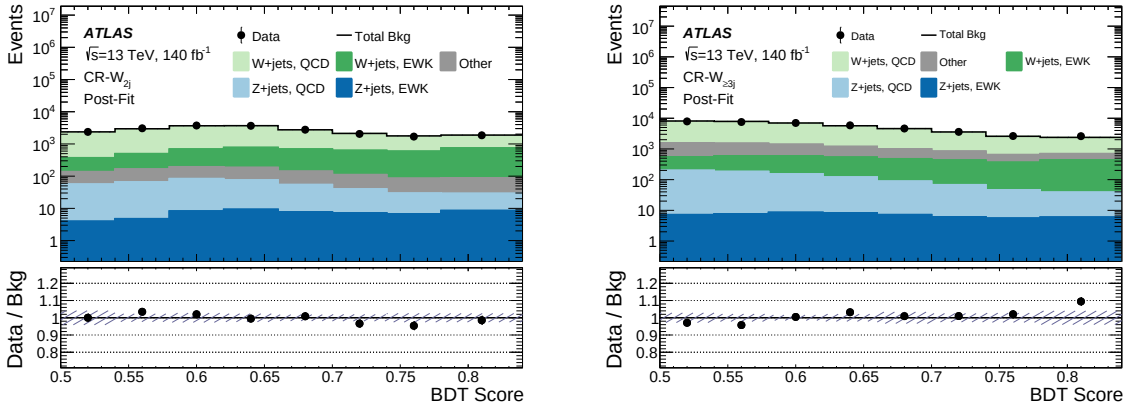

(a)

(b)

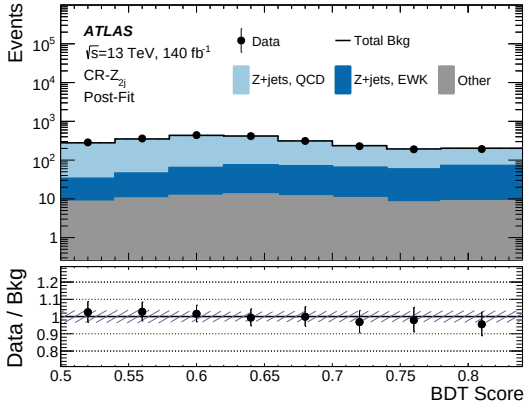

(c)

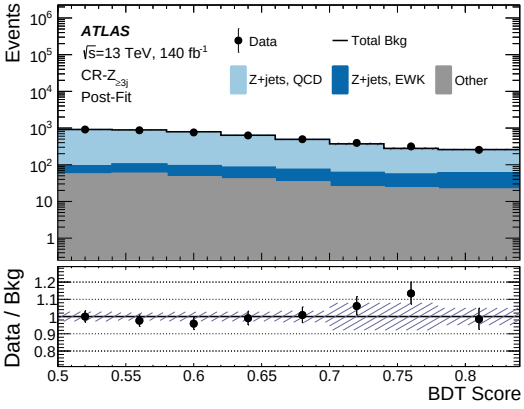

(d)

Figure 3: The BDT score distribution in (a) CR$-W_{2\mathrm{j}}$, (b) CR$-W_{\geq 3\mathrm{j}}$, (c) CR$-Z_{2\mathrm{j}}$, and (d) CR$-Z_{\geq 3\mathrm{j}}$ used to normalise the W + jets and Z + jets estimates. The total background prediction is shown after the fit to the data. The 'Other' category contains rare backgrounds from diboson, triboson and top-quark production processes. The hatched band represents the post-fit experimental, theoretical, and statistical uncertainties in the total background. The bottom panel of each plot shows the ratio between the data and the post-fit background prediction.

$$N_{\text{SR}} = \frac{N^{\text{data}}_{\text{CR-C}} - N^{\text{MC}}_{\text{CR-C}}}{N^{\text{data}}_{\text{CR-B}} - N^{\text{MC}}_{\text{CR-B}}} \left(N^{\text{data}}_{\text{CR-A}} - N^{\text{MC}}_{\text{CR-A}} \right) , \tag{1}$$

where e.g. $N^{\text{data}}_{\text{CR-C}}$ represents the observed data yield in CR-C. Contributions from other SM processes to all three CRs are estimated with MC and subtracted from the data yields, denoted by e.g. $N^{\text{MC}}_{\text{CR-C}}$. A minor dependence of the V + jets normalisation with respect to min $\left(\Delta\phi\left(\mathbf{j}, \mathbf{p}_{\text{T}}^{\text{miss}}\right)\right)$ was found, thus predictions from V + jets are scaled using dedicated one- and two-lepton CRs for which min $\left(\Delta\phi\left(\mathbf{j}, \mathbf{p}_{\text{T}}^{\text{miss}}\right)\right) < 0.4$ before performing the MC subtraction. Except for the lepton requirements, these CRs are otherwise identical to CR-A/B. The obtained multijet predictions in CR-A are binned as a function of the BDT score, using identical binning as in the SR. These vary smoothly as a function of the BDT score, dropping to near zero for BDT scores above 0.84. To mitigate the impact of statistical fluctuations, a χ^2-based fit is performed on the binned multijet estimates using the BDT score as a dependent variable. Several functions were tested to fit the spectrum where a parameterisation via a five-parameter 'Gaussian + linear' function yielded the best results. The final multijet estimates are then taken as the values of the fitted function at the centres of each bin. Tests of this procedure in a region similar to the SR but requiring $220 < E_{\text{T}}^{\text{miss}}/\text{GeV} < 250$ show that this data-driven estimate significantly improves the comparison between predictions and data relative to multijet estimates taken from MC where the latter also suffer from large statistical fluctuations.

7 Systematic uncertainties

Predictions of the BDT score distribution in the signal regions are affected by systematic uncertainties, which are due to both experimental effects and MC generator uncertainties. The V + jets backgrounds are normalised in dedicated control regions such that systematic uncertainties in those backgrounds only affect the extrapolation of the V + jets predictions from the control regions to the signal regions. A summary of all systematic effects is shown in Figure 4.

The trigger, reconstruction, identification and isolation efficiencies for electrons [87] and muons [94], as well as the momentum resolution and scale, primarily affect the signal region through CR$-W$ and CR$-Z$. The uncertainty in the muon reconstruction efficiency was found to be the largest experimental effect on the background yield in the SR as it restricts how precisely the normalisation of the V + jets backgrounds can be determined.

Other sources of experimental systematic uncertainties are the jet energy scale and resolution [95]. The systematic uncertainties related to the modelling of $E_{\text{T}}^{\text{miss}}$ in the simulation are estimated by propagating the uncertainties in the energy and momentum scale of each of the objects entering the calculation, as well as the uncertainties in the soft-term resolution and scale [90].

Several uncertainties arise from MC generator modelling of SM backgrounds. The uncertainties related to the choice of the QCD renormalisation and factorisation scales are assessed by varying the corresponding generator parameters in the matrix element and parton shower up and down by a factor of two around their nominal values, removing combinations where the variations differ by a factor of four. The resulting yield variations for V + jets are approximately 20% for both strong and electroweak V + jets samples before normalisation in the control regions, except for strong V + jets in the 2j regions where variations range from 25% to 45%. An additional uncertainty arises from the scheme, which can be additive, multiplicative, or exponential, used to evaluate NLO electroweak corrections for the strong V + jets backgrounds. The uncertainty in this choice is calculated as the difference in predictions between the scheme that is closest

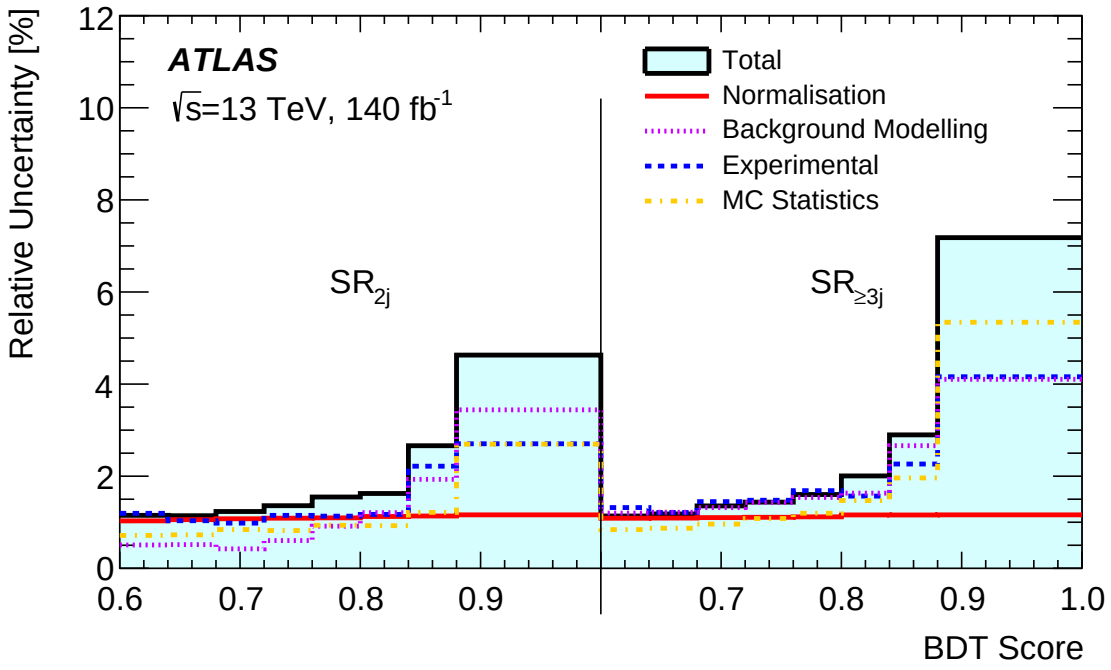

Figure 4: The relative systematic uncertainties in the BDT score distribution for background after the exclusion fit. The 'Normalisation' uncertainty arises from the use of CRs to normalise W + jets and Z + jets, while 'Background Modelling' includes the different sources of theoretical modelling uncertainties in the distribution of BDT scores, as well as the uncertainties in the data-driven multijet background estimate. The uncertainties associated with the measurement of the integrated luminosity as well as the reconstruction and selection of signal leptons, jets and $E_{\mathrm{T}}^{\mathrm{miss}}$ are included under the 'Experimental' category. The 'MC Statistics' uncertainty originates from the limited size of the MC samples used to model the irreducible background contributions. The individual uncertainties can be correlated and do not necessarily add up in quadrature to the total uncertainty.

to the nominal and that which deviates most from nominal. The uncertainties associated with the choice of PDF set, NNPDF [59, 67, 96], and the uncertainty in the strong coupling constant, α_{s}, used in the PDF evaluation are also included. These modelling uncertainties are treated as uncorrelated between the W + jets and Z + jets backgrounds as well as between their strong and electroweak contributions. To take into account imperfect modelling of the minor backgrounds such as top-quark production, a normalisation uncertainty of 30% is added to these in the SRs. The impact of these normalisation uncertainties were found to be below 2% on the final results.

Theoretical uncertainties in the signal predictions include uncertainties in the cross-section and shape uncertainties due to the renormalisation and factorisation scales, choice of PDF set and parton showering. The total cross-section uncertainty was found to be of around 10% and 25% for pure-electroweak and mixed electroweak-QCD production modes at electroweakino mass of 100 GeV, respectively.

Several sources of uncertainty are considered for the multijet background estimate and implemented as individual nuisance parameters. Validation regions with $220 < E_{\mathrm{T}}^{\mathrm{miss}}/\mathrm{GeV} < 250$, i.e. adjacent to CR-A, CR-B, CR-C and CR-D, are used to estimate an uncertainty in the extrapolation from the CR to the SR phase space that is performed in the estimation. The fitted parameters of the Gaussian + linear fit to the BDT distribution in CR-A are varied within their 1σ confidence intervals to generate alternative estimates of the multijet background; the variation leading to the largest deviation of the multijet prediction is used

Table 2: Normalisation factors for W + jets and Z + jets MC samples derived from one- and two-lepton control regions.

Region	CR−W	CR−Z
2j	0.800 ± 0.007	0.829 ± 0.018
≥3j	0.986 ± 0.013	1.046 ± 0.019

to define the fit uncertainty. The impacts of uncertainties on leptons, jets, and $E_{\mathrm{T}}^{\mathrm{miss}}$ as well as theoretical uncertainties in the MC predictions in CR-A, CR-B, CR-C, and CR-D are also considered. As CR-B and CR-C are located within a $E_{\mathrm{T}}^{\mathrm{miss}}$ regime where the $E_{\mathrm{T}}^{\mathrm{miss}}$ trigger might not be fully efficient yet dependent on the event topology, a 5% uncertainty is considered to cover any potential mismodelling of the trigger efficiency in MC simulation. The total pre-fit uncertainty in the multijet background estimate is found to be around 100% in the inclusive $\mathrm{SR}_{2\mathrm{j}}$ and $\mathrm{SR}_{\geq 3\mathrm{j}}$.

As seen in Figure 4, there is no clear dominant source of systematic uncertainty among any of the SR bins; rather, all sources contribute roughly equally to the total uncertainty in the background estimates.

8 Results

Data in the CRs, VRs and SRs are compared with SM predictions using a profile likelihood method [97] implemented in the HistFitter package [98]. Systematic uncertainties are treated as nuisance parameters with Gaussian constraints in the likelihood, where experimental systematic uncertainties are correlated between signal and backgrounds for all regions.

A background-only fit is performed using only CR−W and CR−Z to constrain the normalisation parameters of the W + jets and Z + jets backgrounds. The resulting normalisation parameters are shown in Table 2. With these normalisation parameters applied, the background prediction is checked in VR−W, VR−Z and VR-0L, as shown in Figures 5 and 6, respectively. All VRs are shown separately in the 2j and ≥3j channels. Overall, the predictions agree well with the observed data within the systematic uncertainties, confirming the applicability of the derived V + jets normalisations at large BDT scores and to zero-lepton events. The second bin of VR−$W_{2\mathrm{j}}$ shows a small excess that is slightly below the 2σ level, which is interpreted as a statistical fluctuation of the data. Overall, the deviations between the background predictions and the observed yields in all VRs are within two standard deviations.

To test for the presence of excesses, the background-only fit is extended to include a single-bin signal region consisting of events in either $\mathrm{SR}_{2\mathrm{j}}$ and $\mathrm{SR}_{\geq 3\mathrm{j}}$ with BDT scores greater than 0.88. An independent fit is performed in each single-bin region containing a signal model with an unconstrained normalisation parameter to estimate the contributions of any phenomena beyond those predicted by the SM. Each region is fit simultaneously with the control regions, which are assumed to contain no signal. To quantify the probability under the background-only hypothesis to produce event yields greater than or equal to the observed data, p-values are calculated for each single-bin region. The results of the two fits are shown in Table 3. The lowest p-value is observed in the ≥3j region, corresponding to a significance of less than 1σ. The $\mathrm{CL_s}$ prescription [99] is used to perform a hypothesis test that sets upper limits at the 95% confidence level (CL) on the observed (expected) number of signal events $S^{95}_{\mathrm{obs\,(exp)}}$ in each single-bin region. Dividing S^{95}_{obs} by the integrated luminosity defines the upper limits on the visible cross-sections

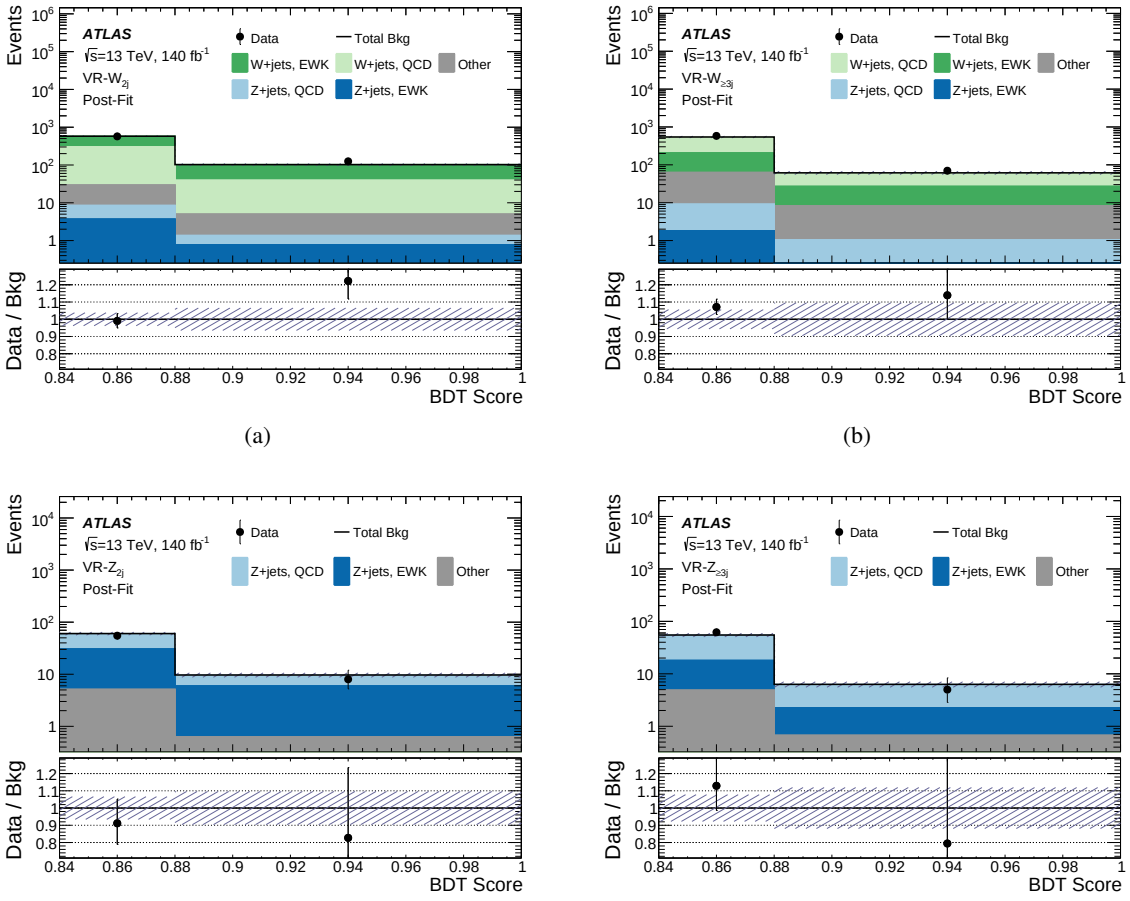

Figure 5: Observed and predicted background distributions of the BDT score in (a) VR$-W_{2j}$, (b) VR$-W_{\geq 3j}$, (c) VR$-Z_{2j}$, and (d) VR$-Z_{\geq 3j}$ validation regions shown after the control region fit. The 'Other' category contains rare backgrounds from diboson, triboson and top-quark production processes. The hatched band represents the post-fit experimental, theoretical, and statistical uncertainties in the total background. The bottom panel of each plot shows the ratio between the data and the post-fit background prediction.

$\langle \epsilon\sigma \rangle^{95}_{\text{obs}}$. Generic non-SM processes that predict more than 13 (25) events in SR_{2j} ($\text{SR}_{\geq 3j}$) with BDT scores greater than 0.88 are excluded at 95% CL, with corresponding upper limits on their visible cross-sections set at 0.09 fb (0.18 fb).

In the absence of significant excesses in these bins, a fit configuration, referred to as the exclusion fit, is formed by extending the background-only fit to include all of the BDT score bins within SR_{2j} and $\text{SR}_{\geq 3j}$. Figure 7 shows the distributions of BDT scores in the signal regions after a fit using this configuration under the assumption that the only contributions are due to SM processes. The corresponding event yields in each SR bin are broken down by process in Tables 4 and 5. The extracted normalisation factors for the V + jets backgrounds in this fit are found to agree within uncertainties with those from the background-only fit that only includes the CRs as constraining regions. Again, no significant excess of events is observed above the SM predictions.

The CL_s prescription in conjunction with the exclusion fit configuration is also used to perform hypothesis

Table 3: Results of the fits in the single-bin signal regions. Left to right: The first column indicates the single-bin SRs under study. The next two columns present observed and expected event yields in the single-bin regions, N_{obs} and N_{exp}. The latter are obtained after the control-region fit, and the errors include both the statistical and systematic uncertainties. The next two columns show the observed 95% CL upper limits on the visible cross-section, $\langle \epsilon\sigma \rangle^{95}_{\text{obs}}$, and on the number of signal events, S^{95}_{obs}. The next column shows the 95% CL upper limit on the number of signal events, S^{95}_{exp}, given the expected number (and $\pm 1\sigma$ deviations from the expectation) of background events. The last column indicates the discovery p-value, $p(s = 0)$.

Single-Bin Region	N_{obs}	N_{exp}	$\langle \epsilon\sigma \rangle^{95}_{\text{obs}}$ [fb]	S^{95}_{obs}	S^{95}_{exp}	$p(s = 0)$
$\text{SR}_{2\text{j}}$	50	55.9 ± 3.7	0.09	13	18^{+7}_{-5}	0.50
$\text{SR}_{\geq 3\text{j}}$	44	39.8 ± 4.3	0.18	25	19^{+9}_{-6}	0.19

Table 4: Observed event yields and fit results for $\text{SR}_{2\text{j}}$ using the exclusion fit. The category 'Other' contains rare backgrounds from diboson, triboson, and top-quark production processes. Uncertainties in the fitted background estimates combine statistical and systematic uncertainties.

BDT Score	[0.60, 0.64)	[0.64, 0.68)	[0.68, 0.72)	[0.72, 0.76)	[0.76, 0.80)	[0.80, 0.84)	[0.84, 0.88)	[0.88, 1.0]
Observed events	3712	2774	1946	1441	1054	729	326	50
Fitted SM events	3590 ± 40	2806 ± 32	1953 ± 24	1490 ± 20	1100 ± 17	774 ± 13	347 ± 9	54.4 ± 2.5
Z + jets, QCD	2104 ± 34	1648 ± 28	1117 ± 22	826 ± 15	576 ± 12	387 ± 10	145 ± 6	16.8 ± 1.1
W + jets, QCD	993 ± 30	691 ± 23	422 ± 18	292 ± 11	190 ± 10	108 ± 7	36.6 ± 3.4	3.7 ± 0.7
Z + jets, EWK	322 ± 8	307 ± 6	273 ± 5	249 ± 5	224 ± 6	192 ± 6	117 ± 5	25.4 ± 1.9
W + jets, EWK	139 ± 3	131 ± 3	117 ± 3	109 ± 3	98 ± 3	79 ± 3	45 ± 2	8.1 ± 0.6
Other	30 ± 7	28 ± 7	23 ± 5	14.0 ± 3.2	12.3 ± 3.0	7.2 ± 1.6	2.8 ± 0.7	0.4 ± 0.1
Multijet	$0.5^{+1.6}_{-0.5}$	$0.6^{+1.9}_{-0.6}$	$0.6^{+1.8}_{-0.6}$	$0.5^{+1.4}_{-0.5}$	$0.3^{+1.0}_{-0.3}$	$0.2^{+0.5}_{-0.2}$	< 0.1	< 0.1

Table 5: Observed event yields and fit results for $\text{SR}_{\geq 3\text{j}}$ using the exclusion fit. The category 'Other' contains rare backgrounds from diboson, triboson, and top-quark production processes. Uncertainties in the fitted background estimates combine statistical and systematic uncertainties.

BDT Score	[0.60, 0.64)	[0.64, 0.68)	[0.68, 0.72)	[0.72, 0.76)	[0.76, 0.80)	[0.80, 0.84)	[0.84, 0.88)	[0.88, 1.0]
Observed events	5504	4295	3068	2358	1611	936	398	44
Fitted SM events	5530 ± 60	4310 ± 50	3120 ± 40	2344 ± 34	1570 ± 25	904 ± 18	358 ± 10	36.6 ± 2.6
Z + jets, QCD	3530 ± 80	2740 ± 60	1980 ± 40	1481 ± 33	974 ± 24	564 ± 18	202 ± 10	21.3 ± 2.1
W + jets, QCD	1390 ± 60	1050 ± 40	708 ± 29	503 ± 21	310 ± 17	138 ± 8	55 ± 5	3.6 ± 0.7
Z + jets, EWK	249 ± 5	226 ± 4	204 ± 5	177 ± 4	154 ± 4	121 ± 4	68 ± 3	6.7 ± 0.8
W + jets, EWK	129 ± 5	111 ± 4	93 ± 3	77 ± 2	56 ± 2	42 ± 2	19 ± 1	2.9 ± 0.4
Other	220 ± 50	170 ± 40	131 ± 30	103 ± 24	74 ± 18	40 ± 10	14 ± 4	2.0 ± 0.5
Multijet	10^{+50}_{-10}	10^{+31}_{-10}	6^{+19}_{-6}	3^{+10}_{-3}	1^{+4}_{-1}	$0.3^{+1.1}_{-0.3}$	< 0.1	$0.1^{+0.4}_{-0.1}$

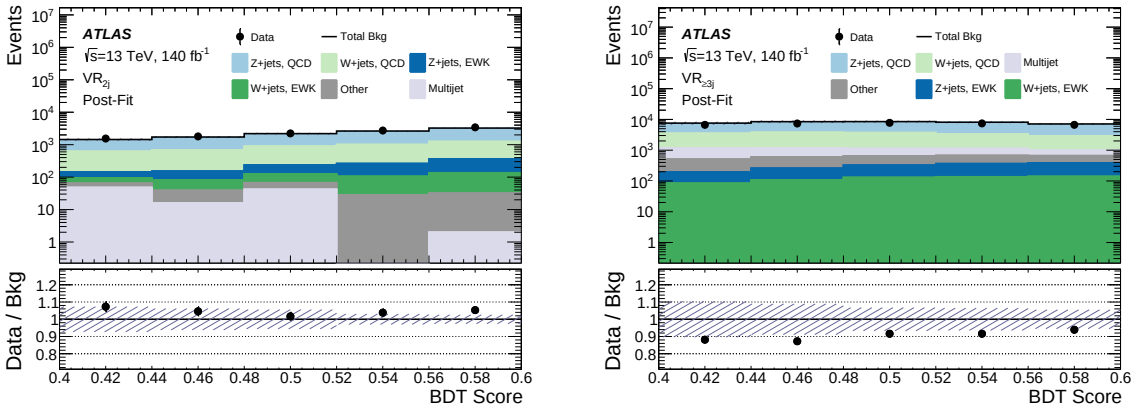

(a) (b)

Figure 6: Observed and predicted background distributions of the BDT score in (a) VR−0L$_{2j}$ and (b) VR−0L$_{\geq 3j}$ low-BDT validation regions, using data-driven estimates for the multijet background. The 'Other' category contains rare backgrounds from diboson, triboson and top-quark production processes. The hatched band represents the post-fit experimental, theoretical, and statistical uncertainties in the total background. The bottom panel of each plot shows the ratio between the data and the post-fit background prediction.

tests of specific SUSY scenarios to set limits on the class of simplified models used to optimise the search. Exclusions at 95% CL are presented in a two-dimensional plane with the horizontal axis given by the mass of the $\widetilde{\chi}_2^0$, and the vertical axis defined by the difference in mass between the $\widetilde{\chi}_2^0$ and $\widetilde{\chi}_1^0$, and are shown in Figure 8. The presented mass limits are restricted to $\Delta m(\widetilde{\chi}_2^0/\widetilde{\chi}_1^\pm, \widetilde{\chi}_1^0) \geq 0.2$ GeV to match the smallest available mass splittings in the simulated signal samples. Since the analysis strategy does not depend on the reconstruction of the $\widetilde{\chi}_2^0/\widetilde{\chi}_1^\pm$ decay products, the results are expected to remain valid for mass splittings below 0.2 GeV as well, assuming that the potentially long lifetime of the $\widetilde{\chi}_1^\pm$ does not degrade the signal acceptance. The observed limit on $\widetilde{\chi}_2^0$ masses for mass splittings below 1 GeV is approximately 117 GeV, depending only slightly on the mass splitting. This is greater than the expected limit of between 100 and 104 GeV for the same $\Delta m(\widetilde{\chi}_2^0/\widetilde{\chi}_1^\pm, \widetilde{\chi}_1^0)$ range due to the mild deficit of observed events in the high BDT score bins of SR$_{2j}$.

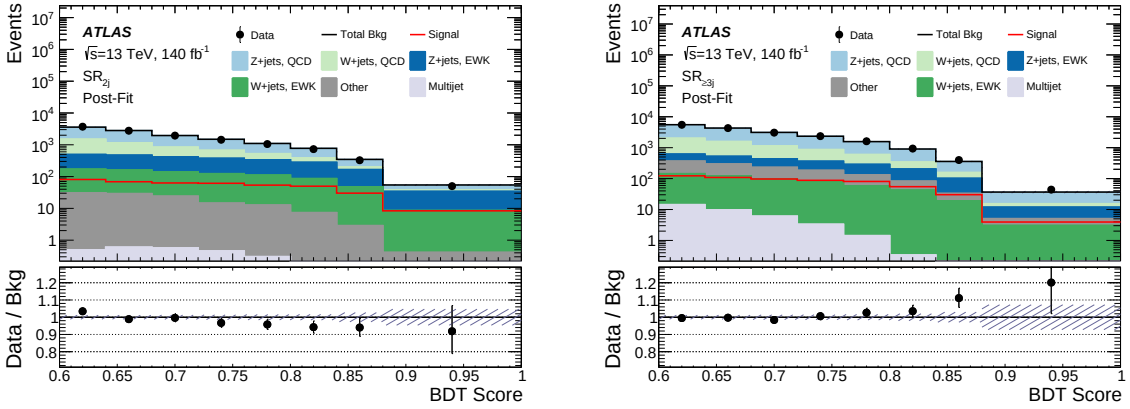

(a) (b)

Figure 7: Observed and predicted background distributions of the BDT score in (a) SR_{2j} and (b) $SR_{\geq 3j}$ after the exclusion fit. The nominal, pre-fit prediction of an example benchmark signal with $(m(\tilde{\chi}_2^0/\tilde{\chi}_1^\pm), m(\tilde{\chi}_1^0)) = (100, 99)$ GeV is shown in red. The 'Other' category contains rare backgrounds from diboson, triboson and top-quark production processes. The hatched band represents the post-fit experimental, theoretical, and statistical uncertainties in the total background. The bottom panel of each plot shows the ratio between the data and the post-fit background prediction.

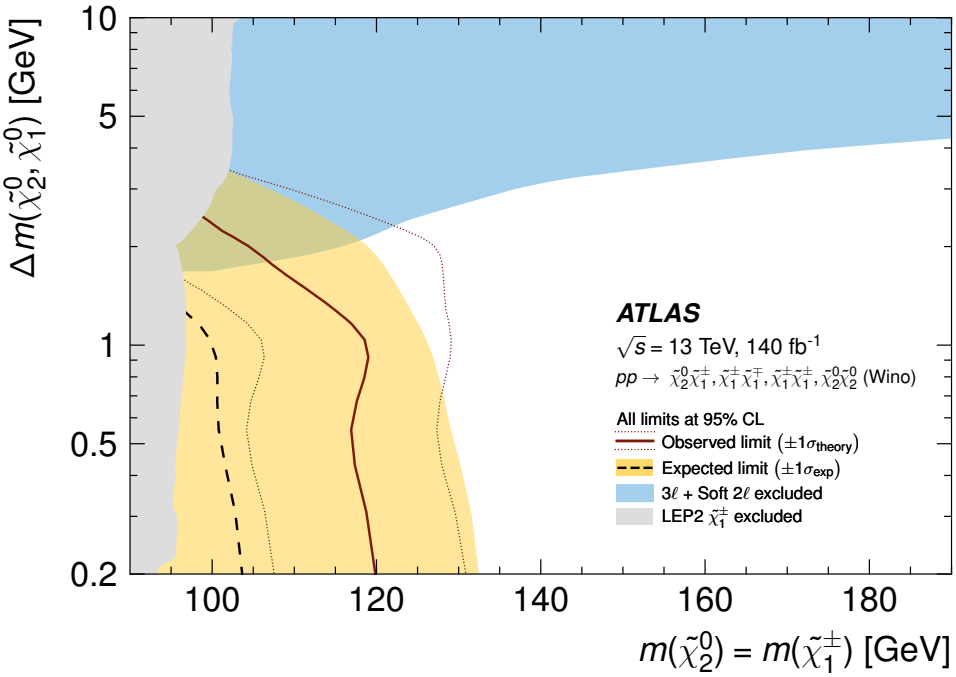

Figure 8: Expected (dashed black line) and observed (solid red line) 95% CL exclusion limits on the compressed SUSY simplified model with a bino-like LSP and wino-like NLSPs being considered. These are shown with $\pm 1\sigma_{\text{exp}}$ (yellow band) from experimental systematic and statistical uncertainties, and with $\pm 1\sigma_{\text{theory}}^{\text{SUSY}}$ (red dotted lines) from signal cross-section uncertainties, respectively. The limits set by the ATLAS searches using the soft lepton [44, 100] signature is illustrated by the blue region while the limit imposed by the LEP experiments [101] is shown in grey.

9 Conclusion

A search for beyond the SM physics is performed using events consistent with the production of invisible particles via VBF processes using $\sqrt{s} = 13$ TeV pp collision data corresponding to an integrated luminosity of 140 fb^{-1} recorded by the ATLAS detector CERN's LHC. The events are required to contain at least two jets with a large separation in pseudorapidity and dijet invariant mass, large missing transverse momentum, and no reconstructed leptons. The events are further classified into two categories that require exactly two or at least three reconstructed jets. Discrimination between SM backgrounds and signal is enhanced by the use of a BDT that is trained on a simplified SUSY model in which a pair of mass-degenerate, wino-like charginos and neutralinos is produced in association with jets before decaying into a close-in-mass ($\Delta m(\widetilde{\chi}_2^0/\widetilde{\chi}_1^\pm, \widetilde{\chi}_1^0) \lesssim 1$ GeV) bino-like neutralino LSP and soft SM particles. This strategy provides unique sensitivity to compressed SUSY scenarios where existing searches relying on soft-lepton signatures become insensitive due to limitations in the reconstruction thresholds for leptons. Unlike those searches, the final state targeted here also allows this search to remain agnostic to the branching ratios of the $\widetilde{\chi}_2^0/\widetilde{\chi}_1^\pm$ decays. The data are found to be consistent with the SM predictions and upper limits are set at 95% CL on the visible cross-section of generic, non-SM processes in the targeted phase space and on the chargino and neutralino masses in a simplified SUSY model featuring wino-like $\widetilde{\chi}_2^0/\widetilde{\chi}_1^\pm$ states that are nearly degenerate in mass with the bino-like $\widetilde{\chi}_1^0$. Including the effects of interference that impact the total signal cross-section and kinematics, a lower limit of 117 GeV is set on the wino-like $\widetilde{\chi}_2^0$ and $\widetilde{\chi}_1^\pm$ masses when they are within 1 GeV of the bino-like $\widetilde{\chi}_1^0$ mass, surpassing previously constraints from the LEP experiment by up to approximately 25 GeV.

Acknowledgements

We thank CERN for the very successful operation of the LHC and its injectors, as well as the support staff at CERN and at our institutions worldwide without whom ATLAS could not be operated efficiently.

The crucial computing support from all WLCG partners is acknowledged gratefully, in particular from CERN, the ATLAS Tier-1 facilities at TRIUMF/SFU (Canada), NDGF (Denmark, Norway, Sweden), CC-IN2P3 (France), KIT/GridKA (Germany), INFN-CNAF (Italy), NL-T1 (Netherlands), PIC (Spain), RAL (UK) and BNL (USA), the Tier-2 facilities worldwide and large non-WLCG resource providers. Major contributors of computing resources are listed in Ref. [102].

We gratefully acknowledge the support of ANPCyT, Argentina; YerPhI, Armenia; ARC, Australia; BMWFW and FWF, Austria; ANAS, Azerbaijan; CNPq and FAPESP, Brazil; NSERC, NRC and CFI, Canada; CERN; ANID, Chile; CAS, MOST and NSFC, China; Minciencias, Colombia; MEYS CR, Czech Republic; DNRF and DNSRC, Denmark; IN2P3-CNRS and CEA-DRF/IRFU, France; SRNSFG, Georgia; BMBF, HGF and MPG, Germany; GSRI, Greece; RGC and Hong Kong SAR, China; ISF and Benoziyo Center, Israel; INFN, Italy; MEXT and JSPS, Japan; CNRST, Morocco; NWO, Netherlands; RCN, Norway; MNiSW, Poland; FCT, Portugal; MNE/IFA, Romania; MSTDI, Serbia; MSSR, Slovakia; ARIS and MVZI, Slovenia; DSI/NRF, South Africa; MICIU/AEI, Spain; SRC and Wallenberg Foundation, Sweden; SERI, SNSF and Cantons of Bern and Geneva, Switzerland; NSTC, Taipei; TENMAK, Türkiye; STFC/UKRI, United Kingdom; DOE and NSF, United States of America.

Individual groups and members have received support from BCKDF, CANARIE, CRC and DRAC, Canada; CERN-CZ, FORTE and PRIMUS, Czech Republic; COST, ERC, ERDF, Horizon 2020, ICSC-

NextGenerationEU and Marie Skłodowska-Curie Actions, European Union; Investissements d'Avenir Labex, Investissements d'Avenir Idex and ANR, France; DFG and AvH Foundation, Germany; Herakleitos, Thales and Aristeia programmes co-financed by EU-ESF and the Greek NSRF, Greece; BSF-NSF and MINERVA, Israel; NCN and NAWA, Poland; La Caixa Banking Foundation, CERCA Programme Generalitat de Catalunya and PROMETEO and GenT Programmes Generalitat Valenciana, Spain; Göran Gustafssons Stiftelse, Sweden; The Royal Society and Leverhulme Trust, United Kingdom.

In addition, individual members wish to acknowledge support from Armenia: Yerevan Physics Institute (FAPERJ); CERN: European Organization for Nuclear Research (CERN PJAS); Chile: Agencia Nacional de Investigación y Desarrollo (FONDECYT 1230812, FONDECYT 1230987, FONDECYT 1240864); China: Chinese Ministry of Science and Technology (MOST-2023YFA1605700), National Natural Science Foundation of China (NSFC - 12175119, NSFC 12275265, NSFC-12075060); Czech Republic: Czech Science Foundation (GACR - 24-11373S), Ministry of Education Youth and Sports (FORTE CZ.02.01.01/00/22_008/0004632), PRIMUS Research Programme (PRIMUS/21/SCI/017); EU: H2020 European Research Council (ERC - 101002463); European Union: European Research Council (ERC - 948254, ERC 101089007), European Union, Future Artificial Intelligence Research (FAIR-NextGenerationEU PE00000013), Italian Center for High Performance Computing, Big Data and Quantum Computing (ICSC, NextGenerationEU); France: Agence Nationale de la Recherche (ANR-20-CE31-0013, ANR-21-CE31-0013, ANR-21-CE31-0022, ANR-22-EDIR-0002); Germany: Baden-Württemberg Stiftung (BW Stiftung-Postdoc Eliteprogramme), Deutsche Forschungsgemeinschaft (DFG - 469666862, DFG - CR 312/5-2); Italy: Istituto Nazionale di Fisica Nucleare (ICSC, NextGenerationEU), Ministero dell'Università e della Ricerca (PRIN - 20223N7F8K - PNRR M4.C2.1.1); Japan: Japan Society for the Promotion of Science (JSPS KAKENHI JP22H01227, JSPS KAKENHI JP22H04944, JSPS KAKENHI JP22KK0227, JSPS KAKENHI JP23KK0245); Netherlands: Netherlands Organisation for Scientific Research (NWO Veni 2020 - VI.Veni.202.179); Norway: Research Council of Norway (RCN-314472); Poland: Ministry of Science and Higher Education (IDUB AGH, POB8, D4 no 9722), Polish National Agency for Academic Exchange (PPN/PPO/2020/1/00002/U/00001), Polish National Science Centre (NCN 2021/42/E/ST2/00350, NCN OPUS nr 2022/47/B/ST2/03059, NCN UMO-2019/34/E/ST2/00393, UMO-2020/37/B/ST2/01043, UMO-2021/40/C/ST2/00187, UMO-2022/47/O/ST2/00148, UMO-2023/49/B/ST2/04085, UMO-2023/51/B/ST2/00920); Slovenia: Slovenian Research Agency (ARIS grant J1-3010); Spain: Generalitat Valenciana (Artemisa, FEDER, IDIFEDER/2018/048), Ministry of Science and Innovation (MCIN & NextGenEU PCI2022-135018-2, MICIN & FEDER PID2021-125273NB, RYC2019-028510-I, RYC2020-030254-I, RYC2021-031273-I, RYC2022-038164-I); Sweden: Swedish Research Council (Swedish Research Council 2023-04654, VR 2018-00482, VR 2022-03845, VR 2022-04683, VR 2023-03403, VR grant 2021-03651), Knut and Alice Wallenberg Foundation (KAW 2018.0458, KAW 2019.0447, KAW 2022.0358); Switzerland: Swiss National Science Foundation (SNSF - PCEFP2_194658); United Kingdom: Leverhulme Trust (Leverhulme Trust RPG-2020-004), Royal Society (NIF-R1-231091); United States of America: U.S. Department of Energy (ECA DE-AC02-76SF00515), Neubauer Family Foundation.

References

[1] ATLAS Collaboration, *Measurement of the cross-section for electroweak production of dijets in association with a Z boson in pp collisions at $\sqrt{s}$ = 13 TeV with the ATLAS detector*, Phys. Lett. B **775** (2017) 206, arXiv: 1709.10264 [hep-ex].

[2] ATLAS Collaboration, *Differential cross-section measurements for the electroweak production of dijets in association with a Z boson in proton–proton collisions at ATLAS*, Eur. Phys. J. C **81** (2021) 163, arXiv: 2006.15458 [hep-ex].

[3] CMS Collaboration, *Measurement of electroweak production of a W boson in association with two jets in proton–proton collisions at $\sqrt{s}$ = 13 TeV*, Eur. Phys. J. C **80** (2020) 43, arXiv: 1903.04040 [hep-ex].

[4] ATLAS Collaboration, *Observation of electroweak $W^{\pm}Z$ boson pair production in association with two jets in pp collisions at $\sqrt{s}$ = 13 TeV with the ATLAS detector*, Phys. Lett. B **793** (2019) 469, arXiv: 1812.09740 [hep-ex].

[5] ATLAS Collaboration, *Evidence for electroweak production of two jets in association with a $Z\gamma$ pair in pp collisions at $\sqrt{s}$ = 13 TeV with the ATLAS detector*, Phys. Lett. B **803** (2020) 135341, arXiv: 1910.09503 [hep-ex].

[6] ATLAS Collaboration, *Observation of electroweak production of two jets and a Z-boson pair*, Nature Phys. **19** (2023) 237, arXiv: 2004.10612 [hep-ex].

[7] CMS Collaboration, *Measurement of the electroweak production of $Z\gamma$ and two jets in proton–proton collisions at $\sqrt{s}$ = 13 TeV and constraints on anomalous quartic gauge couplings*, Phys. Rev. D **104** (2021) 072001, arXiv: 2106.11082 [hep-ex].

[8] CMS Collaboration, *Evidence for WW/WZ vector boson scattering in the decay channel $\ell\nu qq$ produced in association with two jets in proton–proton collisions at $\sqrt{s}$ = 13 TeV*, Phys. Lett. B **834** (2022) 137438, arXiv: 2112.05259 [hep-ex].

[9] CMS Collaboration, *Observation of electroweak W^+W^- pair production in association with two jets in proton–proton collisions at $\sqrt{s}$ = 13 TeV*, Phys. Lett. B **841** (2023) 137495, arXiv: 2205.05711 [hep-ex].

[10] CMS Collaboration, *Measurement of the electroweak production of $W\gamma$ in association with two jets in proton–proton collisions at $\sqrt{s}$ = 13 TeV*, Phys. Rev. D **108** (2023) 032017, arXiv: 2212.12592 [hep-ex].

[11] ATLAS Collaboration, *Measurement and interpretation of same-sign W boson pair production in association with two jets in pp collisions at $\sqrt{s}$ = 13 TeV with the ATLAS detector*, JHEP **04** (2023) 026, arXiv: 2312.00420 [hep-ex].

[12] ATLAS Collaboration, *Fiducial and differential cross-section measurements of electroweak $W\gamma jj$ production in pp collisions at $\sqrt{s}$ = 13 TeV with the ATLAS detector*, (2024), arXiv: 2403.02809 [hep-ex].

[13] ATLAS Collaboration, *Observation of electroweak production of W^+W^- in association with jets in proton–proton collisions at $\sqrt{s}$ = 13 TeV with the ATLAS Detector*, JHEP **07** (2024) 254, arXiv: 2403.04869 [hep-ex].

[14] ATLAS Collaboration, *Evidence for the production of three massive vector bosons with the ATLAS detector*, Phys. Lett. B **798** (2019) 134913, arXiv: 1903.10415 [hep-ex].

[15] CMS Collaboration, *Observation of the production of three massive gauge bosons at $\sqrt{s} = 13$ TeV*, Phys. Rev. Lett. **125** (2020) 151802, arXiv: 2006.11191 [hep-ex].

[16] CMS Collaboration, *Measurements of the $pp \to W^{\pm}\gamma\gamma$ and $pp \to Z\gamma\gamma$ cross sections at $\sqrt{s} = 13$ TeV and limits on anomalous quartic gauge couplings*, JHEP **10** (2021) 174, arXiv: 2105.12780 [hep-ex].

[17] ATLAS Collaboration, *Observation of WWW Production in pp Collisions at $\sqrt{s} = 13$ TeV with the ATLAS Detector*, Phys. Rev. Lett. **129** (2022) 061803, arXiv: 2201.13045 [hep-ex].

[18] ATLAS Collaboration, *Measurement of $Z\gamma\gamma$ production in pp collisions at $\sqrt{s} = 13$ TeV with the ATLAS detector*, Eur. Phys. J. C **83** (2023) 539, arXiv: 2211.14171 [hep-ex].

[19] ATLAS Collaboration, *Observation of $WZ\gamma$ Production in pp Collisions at $\sqrt{s} = 13$ TeV with the ATLAS Detector*, Phys. Rev. Lett. **132** (2024) 021802, arXiv: 2305.16994 [hep-ex].

[20] ATLAS Collaboration, *Observation of $W\gamma\gamma$ triboson production in proton–proton collisions at $\sqrt{s} = 13$ TeV with the ATLAS detector*, Phys. Lett. B **848** (2024) 138400, arXiv: 2308.03041 [hep-ex].

[21] CMS Collaboration, *Observation of $WW\gamma$ Production and Search for $H\gamma$ Production in Proton–Proton Collisions at $\sqrt{s} = 13$ TeV*, Phys. Rev. Lett. **132** (2024) 121901, arXiv: 2310.05164 [hep-ex].

[22] ATLAS Collaboration, *Characterising the Higgs boson with ATLAS data from Run 2 of the LHC*, (2024), arXiv: 2404.05498 [hep-ex].

[23] Y. Golfand and E. Likhtman, *Extension of the Algebra of Poincare Group Generators and Violation of P Invariance*, JETP Lett. **13** (1971) 323, [Pisma Zh. Eksp. Teor. Fiz. **13** (1971) 452].

[24] D. Volkov and V. Akulov, *Is the neutrino a goldstone particle?*, Phys. Lett. B **46** (1973) 109.

[25] J. Wess and B. Zumino, *Supergauge transformations in four dimensions*, Nucl. Phys. B **70** (1974) 39.

[26] J. Wess and B. Zumino, *Supergauge invariant extension of quantum electrodynamics*, Nucl. Phys. B **78** (1974) 1.

[27] S. Ferrara and B. Zumino, *Supergauge invariant Yang-Mills theories*, Nucl. Phys. B **79** (1974) 413.

[28] A. Salam and J. Strathdee, *Super-symmetry and non-Abelian gauges*, Phys. Lett. B **51** (1974) 353.

[29] R. Barbieri and G. Giudice, *Upper bounds on supersymmetric particle masses*, Nucl. Phys. B **306** (1988) 63.

[30] B. de Carlos and J. Casas, *One-loop analysis of the electroweak breaking in supersymmetric models and the fine-tuning problem*, Phys. Lett. B **309** (1993) 320, arXiv: hep-ph/9303291.

[31] K. Griest and D. Seckel, *Three exceptions in the calculation of relic abundances*, Phys. Rev. D **43** (1991) 3191.

[32] J. Edsjö and P. Gondolo, *Neutralino relic density including coannihilations*, Phys. Rev. D **56** (1997) 1879, arXiv: hep-ph/9704361.

[33] G. H. Duan, K.-i. Hikasa, J. Ren, L. Wu and J. M. Yang,
Probing bino-wino coannihilation dark matter below the neutrino floor at the LHC,
Phys. Rev. D **98** (2018) 015010, arXiv: 1804.05238 [hep-ph].

[34] G. R. Farrar and P. Fayet, *Phenomenology of the production, decay, and detection of new hadronic states associated with supersymmetry*, Phys. Lett. B **76** (1978) 575.

[35] H. Goldberg, *Constraint on the Photino Mass from Cosmology*, Phys. Rev. Lett. **50** (1983) 1419, Erratum: Phys. Rev. Lett. **103** (2009) 099905.

[36] J. Ellis, J. S. Hagelin, D. V. Nanopoulos, K. Olive and M. Srednicki,
Supersymmetric relics from the big bang, Nucl. Phys. B **238** (1984) 453.

[37] ATLAS Collaboration, *ATLAS Run 2 searches for electroweak production of supersymmetric particles interpreted within the pMSSM*, JHEP **05** (2024) 106, arXiv: 2402.01392 [hep-ex].

[38] B. Dutta et al.,
Vector Boson Fusion Processes as a Probe of Supersymmetric Electroweak Sectors at the LHC,
Phys. Rev. D **87** (2013) 035029, arXiv: 1210.0964 [hep-ph].

[39] A. G. Delannoy et al., *Probing Dark Matter at the LHC using Vector Boson Fusion Processes*,
Phys. Rev. Lett. **111** (2013) 061801, arXiv: 1304.7779 [hep-ph].

[40] B. Dutta et al., *Probing Compressed Sleptons at the LHC using Vector Boson Fusion Processes*,
Phys. Rev. D **91** (2015) 055025, arXiv: 1411.6043 [hep-ph].

[41] N. Cardona et al.,
Long-term LHC discovery reach for compressed Supersymmetry models using VBF processes,
JHEP **11** (2022) 026, arXiv: 2102.10194 [hep-ph].

[42] CMS Collaboration, *Search for supersymmetry in the vector-boson fusion topology in proton–proton collisions at* $\sqrt{s} = 8$ *TeV*, JHEP **11** (2015) 189, arXiv: 1508.07628 [hep-ex].

[43] CMS Collaboration,
Search for supersymmetry with a compressed mass spectrum in the vector boson fusion topology with 1-lepton and 0-lepton final states in proton–proton collisions at $\sqrt{s} = 13$ *TeV*,
JHEP **08** (2019) 150, arXiv: 1905.13059 [hep-ex].

[44] ATLAS Collaboration, *Searches for electroweak production of supersymmetric particles with compressed mass spectra in* $\sqrt{s} = 13$ *TeV* pp *collisions with the ATLAS detector*,
Phys. Rev. D **101** (2020) 052005, arXiv: 1911.12606 [hep-ex].

[45] ATLAS Collaboration, *Search for invisible Higgs-boson decays in events with vector-boson fusion signatures using* $139\,fb^{-1}$ *of proton–proton data recorded by the ATLAS experiment*,
JHEP **08** (2022) 104, arXiv: 2202.07953 [hep-ex].

[46] CMS Collaboration, *Search for invisible decays of the Higgs boson produced via vector boson fusion in proton–proton collisions at* $\sqrt{s} = 13$ *TeV*, Phys. Rev. D **105** (2022) 092007,
arXiv: 2201.11585 [hep-ex].

[47] ATLAS Collaboration, *Differential cross-sections for events with missing transverse momentum and jets measured with the ATLAS detector in 13 TeV proton-proton collisions*,
JHEP **08** (2024) 223, arXiv: 2403.02793 [hep-ex].

[48] ATLAS Collaboration, *The ATLAS Experiment at the CERN Large Hadron Collider*,
JINST **3** (2008) S08003.

[49] ATLAS Collaboration, *ATLAS Insertable B-Layer: Technical Design Report*, ATLAS-TDR-19; CERN-LHCC-2010-013, 2010, URL: https://cds.cern.ch/record/1291633, Addendum: ATLAS-TDR-19-ADD-1; CERN-LHCC-2012-009, 2012, URL: https://cds.cern.ch/record/1451888.

[50] B. Abbott et al., *Production and integration of the ATLAS Insertable B-Layer*, JINST **13** (2018) T05008, arXiv: 1803.00844 [physics.ins-det].

[51] G. Avoni et al., *The new LUCID-2 detector for luminosity measurement and monitoring in ATLAS*, JINST **13** (2018) P07017.

[52] ATLAS Collaboration, *Performance of the ATLAS trigger system in 2015*, Eur. Phys. J. C **77** (2017) 317, arXiv: 1611.09661 [hep-ex].

[53] ATLAS Collaboration, *Software and computing for Run 3 of the ATLAS experiment at the LHC*, (2024), arXiv: 2404.06335 [hep-ex].

[54] ATLAS Collaboration, *Performance of the missing transverse momentum triggers for the ATLAS detector during Run-2 data taking*, JHEP **08** (2020) 080, arXiv: 2005.09554 [hep-ex].

[55] ATLAS Collaboration, *Performance of electron and photon triggers in ATLAS during LHC Run 2*, Eur. Phys. J. C **80** (2020) 47, arXiv: 1909.00761 [hep-ex].

[56] ATLAS Collaboration, *Performance of the ATLAS muon triggers in Run 2*, JINST **15** (2020) P09015, arXiv: 2004.13447 [physics.ins-det].

[57] ATLAS Collaboration, *Luminosity determination in pp collisions at $\sqrt{s} = 13$ TeV using the ATLAS detector at the LHC*, Eur. Phys. J. C **83** (2023) 982, arXiv: 2212.09379 [hep-ex].

[58] J. Alwall et al., *The automated computation of tree-level and next-to-leading order differential cross sections, and their matching to parton shower simulations*, JHEP **07** (2014) 079, arXiv: 1405.0301 [hep-ph].

[59] NNPDF Collaboration, R. D. Ball et al., *Parton distributions with LHC data*, Nucl. Phys. B **867** (2013) 244, arXiv: 1207.1303 [hep-ph].

[60] T. Sjöstrand et al., *An introduction to PYTHIA 8.2*, Comput. Phys. Commun. **191** (2015) 159, arXiv: 1410.3012 [hep-ph].

[61] ATLAS Collaboration, *ATLAS Pythia 8 tunes to 7 TeV data*, ATL-PHYS-PUB-2014-021, 2014, URL: https://cds.cern.ch/record/1966419.

[62] P. Artoisenet, R. Frederix, O. Mattelaer and R. Rietkerk, *Automatic spin-entangled decays of heavy resonances in Monte Carlo simulations*, JHEP **03** (2013) 015, arXiv: 1212.3460 [hep-ph].

[63] B. C. Allanach et al., *SUSY Les Houches Accord 2*, Comput. Phys. Commun. **180** (2009) 8, arXiv: 0801.0045 [hep-ph].

[64] B. Fuks, M. Klasen, S. Schmiemann and M. Sunder, *Realistic simplified gaugino-higgsino models in the MSSM*, Eur. Phys. J. C **78** (2018) 209, arXiv: 1710.09941 [hep-ph].

[65] J. F. Gunion and H. E. Haber, *Higgs Bosons in Supersymmetric Models (I)*, Nucl. Phys. B **272** (1986) 76, Erratum: Nucl. Phys. B **402** (1993) 567.

[66] E. Bothmann et al., *Event generation with Sherpa 2.2*, SciPost Phys. **7** (2019) 034, arXiv: 1905.09127 [hep-ph].

[67] NNPDF Collaboration, R. D. Ball et al., *Parton distributions for the LHC run II*, JHEP **04** (2015) 040, arXiv: 1410.8849 [hep-ph].

[68] S. Frixione, G. Ridolfi and P. Nason, *A positive-weight next-to-leading-order Monte Carlo for heavy flavour hadroproduction*, JHEP **09** (2007) 126, arXiv: 0707.3088 [hep-ph].

[69] P. Nason, *A new method for combining NLO QCD with shower Monte Carlo algorithms*, JHEP **11** (2004) 040, arXiv: hep-ph/0409146.

[70] S. Frixione, P. Nason and C. Oleari, *Matching NLO QCD computations with parton shower simulations: the POWHEG method*, JHEP **11** (2007) 070, arXiv: 0709.2092 [hep-ph].

[71] S. Alioli, P. Nason, C. Oleari and E. Re, *A general framework for implementing NLO calculations in shower Monte Carlo programs: the POWHEG BOX*, JHEP **06** (2010) 043, arXiv: 1002.2581 [hep-ph].

[72] S. Frixione, E. Laenen, P. Motylinski, C. White and B. R. Webber, *Single-top hadroproduction in association with a W boson*, JHEP **07** (2008) 029, arXiv: 0805.3067 [hep-ph].

[73] T. Sjöstrand, S. Mrenna and P. Skands, *A brief introduction to PYTHIA 8.1*, Comput. Phys. Commun. **178** (2008) 852, arXiv: 0710.3820 [hep-ph].

[74] ATLAS Collaboration, *The Pythia 8 A3 tune description of ATLAS minimum bias and inelastic measurements incorporating the Donnachie–Landshoff diffractive model*, ATL-PHYS-PUB-2016-017, 2016, URL: https://cds.cern.ch/record/2206965.

[75] D. J. Lange, *The EvtGen particle decay simulation package*, Nucl. Instrum. Meth. A **462** (2001) 152.

[76] ATLAS Collaboration, *The ATLAS Simulation Infrastructure*, Eur. Phys. J. C **70** (2010) 823, arXiv: 1005.4568 [physics.ins-det].

[77] S. Agostinelli et al., *GEANT4 – a simulation toolkit*, Nucl. Instrum. Meth. A **506** (2003) 250.

[78] ATLAS Collaboration, *The simulation principle and performance of the ATLAS fast calorimeter simulation FastCaloSim*, ATL-PHYS-PUB-2010-013, 2010, URL: https://cds.cern.ch/record/1300517.

[79] ATLAS Collaboration, *Vertex Reconstruction Performance of the ATLAS Detector at* $\sqrt{s} = 13$ *TeV*, ATL-PHYS-PUB-2015-026, 2015, URL: https://cds.cern.ch/record/2037717.

[80] M. Cacciari, G. P. Salam and G. Soyez, *The anti-k_t jet clustering algorithm*, JHEP **04** (2008) 063, arXiv: 0802.1189 [hep-ph].

[81] M. Cacciari, G. P. Salam and G. Soyez, *FastJet user manual*, Eur. Phys. J. C **72** (2012) 1896, arXiv: 1111.6097 [hep-ph].

[82] ATLAS Collaboration, *Jet reconstruction and performance using particle flow with the ATLAS Detector*, Eur. Phys. J. C **77** (2017) 466, arXiv: 1703.10485 [hep-ex].

[83] ATLAS Collaboration, *Jet energy scale and resolution measured in proton–proton collisions at* $\sqrt{s} = 13$ *TeV with the ATLAS detector*, Eur. Phys. J. C **81** (2021) 689, arXiv: 2007.02645 [hep-ex].

[84] ATLAS Collaboration, *Performance of pile-up mitigation techniques for jets in pp collisions at $\sqrt{s} = 8$ TeV using the ATLAS detector*, Eur. Phys. J. C **76** (2016) 581, arXiv: 1510.03823 [hep-ex].

[85] ATLAS Collaboration, *Forward jet vertex tagging using the particle flow algorithm*, ATL-PHYS-PUB-2019-026, 2019, URL: https://cds.cern.ch/record/2683100.

[86] ATLAS Collaboration, *ATLAS flavour-tagging algorithms for the LHC Run 2 pp collision dataset*, Eur. Phys. J. C **83** (2023) 681, arXiv: 2211.16345 [physics.data-an].

[87] ATLAS Collaboration, *Electron and photon performance measurements with the ATLAS detector using the 2015–2017 LHC proton–proton collision data*, JINST **14** (2019) P12006, arXiv: 1908.00005 [hep-ex].

[88] ATLAS Collaboration, *Electron and photon efficiencies in LHC Run 2 with the ATLAS experiment*, JHEP **05** (2024) 162, arXiv: 2308.13362 [hep-ex].

[89] ATLAS Collaboration, *Muon reconstruction and identification efficiency in ATLAS using the full Run 2 pp collision data set at $\sqrt{s} = 13$ TeV*, Eur. Phys. J. C **81** (2021) 578, arXiv: 2012.00578 [hep-ex].

[90] ATLAS Collaboration, *The performance of missing transverse momentum reconstruction and its significance with the ATLAS detector using $140\,fb^{-1}$ of $\sqrt{s} = 13$ TeV pp collisions*, (2024), arXiv: 2402.05858 [hep-ex].

[91] ATLAS Collaboration, *Characterisation and mitigation of beam-induced backgrounds observed in the ATLAS detector during the 2011 proton–proton run*, JINST **8** (2013) P07004, arXiv: 1303.0223 [hep-ex].

[92] G. Ke et al., *LightGBM: a highly efficient gradient boosting decision tree*, Proceedings of the 31st International Conference on Neural Information Processing Systems (2017) 3149, URL: https://dl.acm.org/doi/10.5555/3294996.3295074.

[93] ATLAS Collaboration, *Object-based missing transverse momentum significance in the ATLAS Detector*, ATLAS-CONF-2018-038, 2018, URL: https://cds.cern.ch/record/2630948.

[94] ATLAS Collaboration, *Muon reconstruction performance of the ATLAS detector in proton–proton collision data at $\sqrt{s} = 13$ TeV*, Eur. Phys. J. C **76** (2016) 292, arXiv: 1603.05598 [hep-ex].

[95] ATLAS Collaboration, *Jet energy scale measurements and their systematic uncertainties in proton–proton collisions at $\sqrt{s} = 13$ TeV with the ATLAS detector*, Phys. Rev. D **96** (2017) 072002, arXiv: 1703.09665 [hep-ex].

[96] J. Butterworth et al., *PDF4LHC recommendations for LHC Run II*, J. Phys. G **43** (2016) 023001, arXiv: 1510.03865 [hep-ph].

[97] G. Cowan, K. Cranmer, E. Gross and O. Vitells, *Asymptotic formulae for likelihood-based tests of new physics*, Eur. Phys. J. C **71** (2011) 1554, arXiv: 1007.1727 [physics.data-an], Erratum: Eur. Phys. J. C **73** (2013) 2501.

[98] M. Baak et al., *HistFitter software framework for statistical data analysis*, Eur. Phys. J. C **75** (2015) 153, arXiv: 1410.1280 [hep-ex].

[99] A. L. Read, *Presentation of search results: the CL_S technique*, J. Phys. G **28** (2002) 2693.

[100] ATLAS Collaboration, *Search for chargino–neutralino pair production in final states with three leptons and missing transverse momentum in* $\sqrt{s} = 13$ *TeV* pp *collisions with the ATLAS detector*, Eur. Phys. J. C **81** (2021) 1118, arXiv: 2106.01676 [hep-ex].

[101] ALEPH, DELPHI, L3, OPAL Experiments,
Combined LEP Chargino Results, up to 208 GeV for low DM, LEPSUSYWG/02-04.1, 2002,
URL: http://lepsusy.web.cern.ch/lepsusy/www/inoslowdmsummer02/charginolowdm_pub.html.

[102] ATLAS Collaboration, *ATLAS Computing Acknowledgements*, ATL-SOFT-PUB-2023-001, 2023,
URL: https://cds.cern.ch/record/2869272.

The ATLAS Collaboration

G. Aad [105], E. Aakvaag [17], B. Abbott [124], S. Abdelhameed [120a], K. Abeling [57], N.J. Abicht [51], S.H. Abidi [30], M. Aboelela [46], A. Aboulhorma [36e], H. Abramowicz [155], H. Abreu [154], Y. Abulaiti [121], B.S. Acharya [71a,71b,k], A. Ackermann [65a], C. Adam Bourdarios [4], L. Adamczyk [88a], S.V. Addepalli [147], M.J. Addison [104], J. Adelman [119], A. Adiguzel [22c], T. Adye [138], A.A. Affolder [140], Y. Afik [41], M.N. Agaras [13], A. Aggarwal [103], C. Agheorghiesei [28c], F. Ahmadov [40,y], S. Ahuja [98], X. Ai [64e], G. Aielli [78a,78b], A. Aikot [168], M. Ait Tamlihat [36e], B. Aitbenchikh [36a], M. Akbiyik [103], T.P.A. Åkesson [101], A.V. Akimov [149], D. Akiyama [173], N.N. Akolkar [25], S. Aktas [22a], K. Al Khoury [43], G.L. Alberghi [24b], J. Albert [170], P. Albicocco [55], G.L. Albouy [62], S. Alderweireldt [54], Z.L. Alegria [125], M. Aleksa [37], I.N. Aleksandrov [40], C. Alexa [28b], T. Alexopoulos [10], F. Alfonsi [24b], M. Algren [58], M. Alhroob [172], B. Ali [136], H.M.J. Ali [94,s], S. Ali [32], S.W. Alibocus [95], M. Aliev [34c], G. Alimonti [73a], W. Alkakhi [57], C. Allaire [68], B.M.M. Allbrooke [150], J.S. Allen [104], J.F. Allen [54], C.A. Allendes Flores [141f], P.P. Allport [21], A. Aloisio [74a,74b], F. Alonso [93], C. Alpigiani [142], Z.M.K. Alsolami [94], M. Alvarez Estevez [102], A. Alvarez Fernandez [103], M. Alves Cardoso [58], M.G. Alviggi [74a,74b], M. Aly [104], Y. Amaral Coutinho [85b], A. Ambler [107], C. Amelung[37], M. Amerl [104], C.G. Ames [112], D. Amidei [109], B. Amini [56], K.J. Amirie [159], S.P. Amor Dos Santos [134a], K.R. Amos [168], D. Amperiadou [156], S. An[86], V. Ananiev [129], C. Anastopoulos [143], T. Andeen [11], J.K. Anders [37], A.C. Anderson [61], S.Y. Andrean [49a,49b], A. Andreazza [73a,73b], S. Angelidakis [9], A. Angerami [43], A.V. Anisenkov [39], A. Annovi [76a], C. Antel [58], E. Antipov [149], M. Antonelli [55], F. Anulli [77a], M. Aoki [86], T. Aoki [157], M.A. Aparo [150], L. Aperio Bella [50], C. Appelt [155], A. Apyan [27], S.J. Arbiol Val [89], C. Arcangeletti [55], A.T.H. Arce [53], J-F. Arguin [111], S. Argyropoulos [156], J.-H. Arling [50], O. Arnaez [4], H. Arnold [149], G. Artoni [77a,77b], H. Asada [114], K. Asai [122], S. Asai [157], N.A. Asbah [37], R.A. Ashby Pickering [172], K. Assamagan [30], R. Astalos [29a], K.S.V. Astrand [101], S. Atashi [163], R.J. Atkin [34a], H. Atmani[36f], P.A. Atmasiddha [132], K. Augsten [136], A.D. Auriol [21], V.A. Austrup [104], G. Avolio [37], K. Axiotis [58], G. Azuelos [111,ac], D. Babal [29b], H. Bachacou [139], K. Bachas [156,o], A. Bachiu [35], E. Bachmann[52], A. Badea [41], T.M. Baer [109], P. Bagnaia [77a,77b], M. Bahmani [19], D. Bahner [56], K. Bai [127], J.T. Baines [138], L. Baines [97], O.K. Baker [177], E. Bakos [16], D. Bakshi Gupta [8], L.E. Balabram Filho [85b], V. Balakrishnan [124], R. Balasubramanian [4], E.M. Baldin [39], P. Balek [88a], E. Ballabene [24b,24a], F. Balli [139], L.M. Baltes [65a], W.K. Balunas [33], J. Balz [103], I. Bamwidhi [120b], E. Banas [89], M. Bandieramonte [133], A. Bandyopadhyay [25], S. Bansal [25], L. Barak [155], M. Barakat [50], E.L. Barberio [108], D. Barberis [59b,59a], M. Barbero [105], M.Z. Barel [118], T. Barillari [113], M-S. Barisits [37], T. Barklow [147], P. Baron [126], D.A. Baron Moreno [104], A. Baroncelli [64a], A.J. Barr [130], J.D. Barr [99], F. Barreiro [102], J. Barreiro Guimarães da Costa [14], M.G. Barros Teixeira [134a], S. Barsov [39], F. Bartels [65a], R. Bartoldus [147], A.E. Barton [94], P. Bartos [29a], A. Basan [103], M. Baselga [51], A. Bassalat [68,b], M.J. Basso [160a], S. Bataju [46], R. Bate [169], R.L. Bates [61], S. Batlamous[102], B. Batool [145], M. Battaglia [140], D. Battulga [19], M. Bauce [77a,77b], M. Bauer [81], P. Bauer [25], L.T. Bazzano Hurrell [31], J.B. Beacham [53], T. Beau [131], J.Y. Beaucamp [93], P.H. Beauchemin [162], P. Bechtle [25], H.P. Beck [20,n], K. Becker [172], A.J. Beddall [84], V.A. Bednyakov [40], C.P. Bee [149], L.J. Beemster [16], T.A. Beermann [37], M. Begalli [85d], M. Begel [30], A. Behera [149], J.K. Behr [50], J.F. Beirer [37], F. Beisiegel [25], M. Belfkir [120b], G. Bella [155], L. Bellagamba [24b], A. Bellerive [35], P. Bellos [21], K. Beloborodov [39], D. Benchekroun [36a], F. Bendebba [36a], Y. Benhammou [155],

K.C. Benkendorfer[63], L. Beresford[50], M. Beretta[55], E. Bergeaas Kuutmann[166], N. Berger[4], B. Bergmann[136], J. Beringer[18a], G. Bernardi[5], C. Bernius[147], F.U. Bernlochner[25], F. Bernon[37], A. Berrocal Guardia[13], T. Berry[98], P. Berta[137], A. Berthold[52], S. Bethke[113], A. Betti[77a,77b], A.J. Bevan[97], N.K. Bhalla[56], S. Bhatta[149], D.S. Bhattacharya[171], P. Bhattarai[147], Z.M. Bhatti[121], K.D. Bhide[56], V.S. Bhopatkar[125], R.M. Bianchi[133], G. Bianco[24b,24a], O. Biebel[112], M. Biglietti[79a], C.S. Billingsley[46], Y. Bimgdi[36f], M. Bindi[57], A. Bingul[22b], C. Bini[77a,77b], G.A. Bird[33], M. Birman[174], M. Biros[137], S. Biryukov[150], T. Bisanz[51], E. Bisceglie[45b,45a], J.P. Biswal[138], D. Biswas[145], I. Bloch[50], A. Blue[61], U. Blumenschein[97], J. Blumenthal[103], V.S. Bobrovnikov[39], M. Boehler[56], B. Boehm[171], D. Bogavac[37], A.G. Bogdanchikov[39], L.S. Boggia[131], C. Bohm[49a], V. Boisvert[98], P. Bokan[37], T. Bold[88a], M. Bomben[5], M. Bona[97], M. Boonekamp[139], A.G. Borbély[61], I.S. Bordulev[39], G. Borissov[94], D. Bortoletto[130], D. Boscherini[24b], M. Bosman[13], K. Bouaouda[36a], N. Bouchhar[168], L. Boudet[4], J. Boudreau[133], E.V. Bouhova-Thacker[94], D. Boumediene[42], R. Bouquet[59b,59a], A. Boveia[123], J. Boyd[37], D. Boye[30], I.R. Boyko[40], L. Bozianu[58], J. Bracinik[21], N. Brahimi[4], G. Brandt[176], O. Brandt[33], B. Brau[106], J.E. Brau[127], R. Brener[174], L. Brenner[118], R. Brenner[166], S. Bressler[174], G. Brianti[80a,80b], D. Britton[61], D. Britzger[113], I. Brock[25], R. Brock[110], G. Brooijmans[43], A.J. Brooks[70], E.M. Brooks[160b], E. Brost[30], L.M. Brown[170], L.E. Bruce[63], T.L. Bruckler[130], P.A. Bruckman de Renstrom[89], B. Brüers[50], A. Bruni[24b], G. Bruni[24b], D. Brunner[49a,49b], M. Bruschi[24b], N. Bruscino[77a,77b], T. Buanes[17], Q. Buat[142], D. Buchin[113], A.G. Buckley[61], O. Bulekov[39], B.A. Bullard[147], S. Burdin[95], C.D. Burgard[51], A.M. Burger[37], B. Burghgrave[8], O. Burlayenko[56], J. Burleson[167], J.T.P. Burr[33], J.C. Burzynski[146], E.L. Busch[43], V. Büscher[103], P.J. Bussey[61], J.M. Butler[26], C.M. Buttar[61], J.M. Butterworth[99], W. Buttinger[138], C.J. Buxo Vazquez[110], A.R. Buzykaev[39], S. Cabrera Urbán[168], L. Cadamuro[68], D. Caforio[60], H. Cai[133], Y. Cai[14,115c], Y. Cai[115a], V.M.M. Cairo[37], O. Cakir[3a], N. Calace[37], P. Calafiura[18a], G. Calderini[131], P. Calfayan[35], G. Callea[61], L.P. Caloba[85b], D. Calvet[42], S. Calvet[42], R. Camacho Toro[131], S. Camarda[37], D. Camarero Munoz[27], P. Camarri[78a,78b], M.T. Camerlingo[74a,74b], D. Cameron[37], C. Camincher[170], M. Campanelli[99], A. Camplani[44], V. Canale[74a,74b], A.C. Canbay[3a], E. Canonero[98], J. Cantero[168], Y. Cao[167], F. Capocasa[27], M. Capua[45b,45a], A. Carbone[73a,73b], R. Cardarelli[78a], J.C.J. Cardenas[8], M.P. Cardiff[27], G. Carducci[45b,45a], T. Carli[37], G. Carlino[74a], J.I. Carlotto[13], B.T. Carlson[133,p], E.M. Carlson[170,160a], J. Carmignani[95], L. Carminati[73a,73b], A. Carnelli[139], M. Carnesale[37], S. Caron[117], E. Carquin[141f], I.B. Carr[108], S. Carrá[73a], G. Carratta[24b,24a], A.M. Carroll[127], M.P. Casado[13,h], M. Caspar[50], F.L. Castillo[4], L. Castillo Garcia[13], V. Castillo Gimenez[168], N.F. Castro[134a,134e], A. Catinaccio[37], J.R. Catmore[129], T. Cavaliere[4], V. Cavaliere[30], L.J. Caviedes Betancourt[23b], Y.C. Cekmecelioglu[50], E. Celebi[84], S. Cella[37], V. Cepaitis[58], K. Cerny[126], A.S. Cerqueira[85a], A. Cerri[150], L. Cerrito[78a,78b], F. Cerutti[18a], B. Cervato[145], A. Cervelli[24b], G. Cesarini[55], S.A. Cetin[84], P.M. Chabrillat[131], D. Chakraborty[119], J. Chan[18a], W.Y. Chan[157], J.D. Chapman[33], E. Chapon[139], B. Chargeishvili[153b], D.G. Charlton[21], M. Chatterjee[20], C. Chauhan[137], Y. Che[115a], S. Chekanov[6], S.V. Chekulaev[160a], G.A. Chelkov[40,a], A. Chen[109], B. Chen[155], B. Chen[170], H. Chen[115a], H. Chen[30], J. Chen[64c], J. Chen[146], M. Chen[130], S. Chen[90], S.J. Chen[115a], X. Chen[64c], X. Chen[15,ab], Y. Chen[64a], C.L. Cheng[175], H.C. Cheng[66a], S. Cheong[147], A. Cheplakov[40], E. Cheremushkina[50], E. Cherepanova[118], R. Cherkaoui El Moursli[36e], E. Cheu[7], K. Cheung[67], L. Chevalier[139], V. Chiarella[55], G. Chiarelli[76a], N. Chiedde[105], G. Chiodini[72a], A.S. Chisholm[21], A. Chitan[28b], M. Chitishvili[168], M.V. Chizhov[40,q], K. Choi[11], Y. Chou[142],

E.Y.S. Chow [117], K.L. Chu [174], M.C. Chu [66a], X. Chu [14,115c], Z. Chubinidze [55], J. Chudoba [135], J.J. Chwastowski [89], D. Cieri [113], K.M. Ciesla [88a], V. Cindro [96], A. Ciocio [18a], F. Cirotto [74a,74b], Z.H. Citron [174], M. Citterio [73a], D.A. Ciubotaru[28b], A. Clark [58], P.J. Clark [54], N. Clarke Hall [99], C. Clarry [159], J.M. Clavijo Columbie [50], S.E. Clawson [50], C. Clement [49a,49b], Y. Coadou [105], M. Cobal [71a,71c], A. Coccaro [59b], R.F. Coelho Barrue [134a], R. Coelho Lopes De Sa [106], S. Coelli [73a], L.S. Colangeli [159], B. Cole [43], J. Collot [62], P. Conde Muiño [134a,134g], M.P. Connell [34c], S.H. Connell [34c], E.I. Conroy [130], F. Conventi [74a,ad], H.G. Cooke [21], A.M. Cooper-Sarkar [130], F.A. Corchia [24b,24a], A. Cordeiro Oudot Choi [131], L.D. Corpe [42], M. Corradi [77a,77b], F. Corriveau [107,x], A. Cortes-Gonzalez [19], M.J. Costa [168], F. Costanza [4], D. Costanzo [143], B.M. Cote [123], J. Couthures [4], G. Cowan [98], K. Cranmer [175], L. Cremer [51], D. Cremonini [24b,24a], S. Crépé-Renaudin [62], F. Crescioli [131], M. Cristinziani [145], M. Cristoforetti [80a,80b], V. Croft [118], J.E. Crosby [125], G. Crosetti [45b,45a], A. Cueto [102], H. Cui [99], Z. Cui [7], W.R. Cunningham [61], F. Curcio [168], J.R. Curran [54], P. Czodrowski [37], M.J. Da Cunha Sargedas De Sousa [59b,59a], J.V. Da Fonseca Pinto [85b], C. Da Via [104], W. Dabrowski [88a], T. Dado [37], S. Dahbi [152], T. Dai [109], D. Dal Santo [20], C. Dallapiccola [106], M. Dam [44], G. D'amen [30], V. D'Amico [112], J. Damp [103], J.R. Dandoy [35], D. Dannheim [37], M. Danninger [146], V. Dao [149], G. Darbo [59b], S.J. Das [30], F. Dattola [50], S. D'Auria [73a,73b], A. D'Avanzo [74a,74b], C. David [34a], T. Davidek [137], I. Dawson [97], H.A. Day-hall [136], K. De [8], C. De Almeida Rossi [159], R. De Asmundis [74a], N. De Biase [50], S. De Castro [24b,24a], N. De Groot [117], P. de Jong [118], H. De la Torre [119], A. De Maria [115a], A. De Salvo [77a], U. De Sanctis [78a,78b], F. De Santis [72a,72b], A. De Santo [150], J.B. De Vivie De Regie [62], J. Debevc [96], D.V. Dedovich[40], J. Degens [95], A.M. Deiana [46], F. Del Corso [24b,24a], J. Del Peso [102], L. Delagrange [131], F. Deliot [139], C.M. Delitzsch [51], M. Della Pietra [74a,74b], D. Della Volpe [58], A. Dell'Acqua [37], L. Dell'Asta [73a,73b], M. Delmastro [4], C.C. Delogu [103], P.A. Delsart [62], S. Demers [177], M. Demichev [40], S.P. Denisov [39], L. D'Eramo [42], D. Derendarz [89], F. Derue [131], P. Dervan [95], K. Desch [25], C. Deutsch [25], F.A. Di Bello [59b,59a], A. Di Ciaccio [78a,78b], L. Di Ciaccio [4], A. Di Domenico [77a,77b], C. Di Donato [74a,74b], A. Di Girolamo [37], G. Di Gregorio [37], A. Di Luca [80a,80b], B. Di Micco [79a,79b], R. Di Nardo [79a,79b], K.F. Di Petrillo [41], M. Diamantopoulou [35], F.A. Dias [118], T. Dias Do Vale [146], M.A. Diaz [141a,141b], A.R. Didenko [40], M. Didenko [168], E.B. Diehl [109], S. Díez Cornell [50], C. Diez Pardos [145], C. Dimitriadi [166], A. Dimitrievska [21], J. Dingfelder [25], T. Dingley [130], I-M. Dinu [28b], S.J. Dittmeier [65b], F. Dittus [37], M. Divisek [137], B. Dixit [95], F. Djama [105], T. Djobava [153b], C. Doglioni [104,101], A. Dohnalova [29a], Z. Dolezal [137], K. Domijan [88a], K.M. Dona [41], M. Donadelli [85d], B. Dong [110], J. Donini [42], A. D'Onofrio [74a,74b], M. D'Onofrio [95], J. Dopke [138], A. Doria [74a], N. Dos Santos Fernandes [134a], P. Dougan [104], M.T. Dova [93], A.T. Doyle [61], M.A. Draguet [130], M.P. Drescher [57], E. Dreyer [174], I. Drivas-koulouris [10], M. Drnevich [121], M. Drozdova [58], D. Du [64a], T.A. du Pree [118], F. Dubinin [39], M. Dubovsky [29a], E. Duchovni [174], G. Duckeck [112], O.A. Ducu [28b], D. Duda [54], A. Dudarev [37], E.R. Duden [27], M. D'uffizi [104], L. Duflot [68], M. Dührssen [37], I. Duminica [28g], A.E. Dumitriu [28b], M. Dunford [65a], S. Dungs [51], K. Dunne [49a,49b], A. Duperrin [105], H. Duran Yildiz [3a], M. Düren [60], A. Durglishvili [153b], B.L. Dwyer [119], G.I. Dyckes [18a], M. Dyndal [88a], B.S. Dziedzic [37], Z.O. Earnshaw [150], G.H. Eberwein [130], B. Eckerova [29a], S. Eggebrecht [57], E. Egidio Purcino De Souza [85e], L.F. Ehrke [58], G. Eigen [17], K. Einsweiler [18a], T. Ekelof [166], P.A. Ekman [101], S. El Farkh [36b], Y. El Ghazali [64a], H. El Jarrari [37], A. El Moussaouy [36a], V. Ellajosyula [166], M. Ellert [166], F. Ellinghaus [176], N. Ellis [37], J. Elmsheuser [30], M. Elsawy [120a], M. Elsing [37], D. Emeliyanov [138], Y. Enari [86], I. Ene [18a], S. Epari [13], P.A. Erland [89], D. Ernani Martins Neto [89], M. Errenst [176], M. Escalier [68], C. Escobar [168], E. Etzion [155],

G. Evans [134a], H. Evans [70], L.S. Evans [98], A. Ezhilov [39], S. Ezzarqtouni [36a], F. Fabbri [24b,24a], L. Fabbri [24b,24a], G. Facini [99], V. Fadeyev [140], R.M. Fakhrutdinov [39], D. Fakoudis [103], S. Falciano [77a], L.F. Falda Ulhoa Coelho [134a], F. Fallavollita [113], G. Falsetti [45b,45a], J. Faltova [137], C. Fan [167], K.Y. Fan [66b], Y. Fan [14], Y. Fang [14,115c], M. Fanti [73a,73b], M. Faraj [71a,71b], Z. Farazpay [100], A. Farbin [8], A. Farilla [79a], T. Farooque [110], J.N. Farr [177], S.M. Farrington [138,54], F. Fassi [36e], D. Fassouliotis [9], M. Faucci Giannelli [78a,78b], W.J. Fawcett [33], L. Fayard [68], P. Federic [137], P. Federicova [135], O.L. Fedin [39,a], M. Feickert [175], L. Feligioni [105], D.E. Fellers [127], C. Feng [64b], Z. Feng [118], M.J. Fenton [163], L. Ferencz [50], R.A.M. Ferguson [94], P. Fernandez Martinez [69], M.J.V. Fernoux [105], J. Ferrando [94], A. Ferrari [166], P. Ferrari [118,117], R. Ferrari [75a], D. Ferrere [58], C. Ferretti [109], M.P. Fewell [1], D. Fiacco [77a,77b], F. Fiedler [103], P. Fiedler [136], S. Filimonov [39], A. Filipčič [96], E.K. Filmer [160a], F. Filthaut [117], M.C.N. Fiolhais [134a,134c,c], L. Fiorini [168], W.C. Fisher [110], T. Fitschen [104], P.M. Fitzhugh [139], I. Fleck [145], P. Fleischmann [109], T. Flick [176], M. Flores [34d,z], L.R. Flores Castillo [66a], L. Flores Sanz De Acedo [37], F.M. Follega [80a,80b], N. Fomin [33], J.H. Foo [159], A. Formica [139], A.C. Forti [104], E. Fortin [37], A.W. Fortman [18a], M.G. Foti [18a], L. Fountas [9,i], D. Fournier [68], H. Fox [94], P. Francavilla [76a,76b], S. Francescato [63], S. Franchellucci [58], M. Franchini [24b,24a], S. Franchino [65a], D. Francis [37], L. Franco [117], V. Franco Lima [37], L. Franconi [50], M. Franklin [63], G. Frattari [27], Y.Y. Frid [155], J. Friend [61], N. Fritzsche [37], A. Froch [58], D. Froidevaux [37], J.A. Frost [130], Y. Fu [64a], S. Fuenzalida Garrido [141f], M. Fujimoto [105], K.Y. Fung [66a], E. Furtado De Simas Filho [85e], M. Furukawa [157], J. Fuster [168], A. Gaa [57], A. Gabrielli [24b,24a], A. Gabrielli [159], P. Gadow [37], G. Gagliardi [59b,59a], L.G. Gagnon [18a], S. Gaid [165], S. Galantzan [155], J. Gallagher [1], E.J. Gallas [130], A.L. Gallen [166], B.J. Gallop [138], K.K. Gan [123], S. Ganguly [157], Y. Gao [54], F.M. Garay Walls [141a,141b], B. Garcia [30], C. García [168], A. Garcia Alonso [118], A.G. Garcia Caffaro [177], J.E. García Navarro [168], M. Garcia-Sciveres [18a], G.L. Gardner [132], R.W. Gardner [41], N. Garelli [162], R.B. Garg [147], J.M. Gargan [54], C.A. Garner [159], C.M. Garvey [34a], V.K. Gassmann [162], G. Gaudio [75a], V. Gautam [13], P. Gauzzi [77a,77b], J. Gavranovic [96], I.L. Gavrilenko [39], A. Gavrilyuk [39], C. Gay [169], G. Gaycken [127], E.N. Gazis [10], A.A. Geanta [28b], A. Gekow [123], C. Gemme [59b], M.H. Genest [62], A.D. Gentry [116], S. George [98], W.F. George [21], T. Geralis [48], A.A. Gerwin [124], P. Gessinger-Befurt [37], M.E. Geyik [176], M. Ghani [172], K. Ghorbanian [97], A. Ghosal [145], A. Ghosh [163], A. Ghosh [7], B. Giacobbe [24b], S. Giagu [77a,77b], T. Giani [118], A. Giannini [64a], S.M. Gibson [98], M. Gignac [140], D.T. Gil [88b], A.K. Gilbert [88a], B.J. Gilbert [43], D. Gillberg [35], G. Gilles [118], L. Ginabat [131], D.M. Gingrich [2,ac], M.P. Giordani [71a,71c], P.F. Giraud [139], G. Giugliarelli [71a,71c], D. Giugni [73a], F. Giuli [78a,78b], I. Gkialas [9,i], L.K. Gladilin [39], C. Glasman [102], G.R. Gledhill [127], G. Glemža [50], M. Glisic [127], I. Gnesi [45b], Y. Go [30], M. Goblirsch-Kolb [37], B. Gocke [51], D. Godin [111], B. Gokturk [22a], S. Goldfarb [108], T. Golling [58], M.G.D. Gololo [34g], D. Golubkov [39], J.P. Gombas [110], A. Gomes [134a,134b], G. Gomes Da Silva [145], A.J. Gomez Delegido [168], R. Gonçalo [134a], L. Gonella [21], A. Gongadze [153c], F. Gonnella [21], J.L. Gonski [147], R.Y. González Andana [54], S. González de la Hoz [168], R. Gonzalez Lopez [95], C. Gonzalez Renteria [18a], M.V. Gonzalez Rodrigues [50], R. Gonzalez Suarez [166], S. Gonzalez-Sevilla [58], L. Goossens [37], B. Gorini [37], E. Gorini [72a,72b], A. Gorišek [96], T.C. Gosart [132], A.T. Goshaw [53], M.I. Gostkin [40], S. Goswami [125], C.A. Gottardo [37], S.A. Gotz [112], M. Gouighri [36b], V. Goumarre [50], A.G. Goussiou [142], N. Govender [34c], R.P. Grabarczyk [130], I. Grabowska-Bold [88a], K. Graham [35], E. Gramstad [129], S. Grancagnolo [72a,72b], C.M. Grant [1,139], P.M. Gravila [28f], F.G. Gravili [72a,72b], H.M. Gray [18a], M. Greco [72a,72b], M.J. Green [1], C. Grefe [25], A.S. Grefsrud [17], I.M. Gregor [50], K.T. Greif [163], P. Grenier [147], S.G. Grewe [113], A.A. Grillo [140], K. Grimm [32], S. Grinstein [13,t], J.-F. Grivaz [68],

E. Gross[174], J. Grosse-Knetter[57], L. Guan[109], J.G.R. Guerrero Rojas[168], G. Guerrieri[37], R. Gugel[103], J.A.M. Guhit[109], A. Guida[19], E. Guilloton[172], S. Guindon[37], F. Guo[14,115c], J. Guo[64c], L. Guo[50], L. Guo[14], Y. Guo[109], A. Gupta[51], R. Gupta[133], S. Gurbuz[25], S.S. Gurdasani[56], G. Gustavino[77a,77b], P. Gutierrez[124], L.F. Gutierrez Zagazeta[132], M. Gutsche[52], C. Gutschow[99], C. Gwenlan[130], C.B. Gwilliam[95], E.S. Haaland[129], A. Haas[121], M. Habedank[61], C. Haber[18a], H.K. Hadavand[8], A. Hadef[52], A.I. Hagan[94], J.J. Hahn[145], E.H. Haines[99], M. Haleem[171], J. Haley[125], G.D. Hallewell[105], L. Halser[20], K. Hamano[170], M. Hamer[25], E.J. Hampshire[98], J. Han[64b], L. Han[115a], L. Han[64a], S. Han[18a], Y.F. Han[159], K. Hanagaki[86], M. Hance[140], D.A. Hangal[43], H. Hanif[146], M.D. Hank[132], J.B. Hansen[44], P.H. Hansen[44], D. Harada[58], T. Harenberg[176], S. Harkusha[178], M.L. Harris[106], Y.T. Harris[25], J. Harrison[13], N.M. Harrison[123], P.F. Harrison[172], N.M. Hartman[113], N.M. Hartmann[112], R.Z. Hasan[98,138], Y. Hasegawa[144], F. Haslbeck[130], S. Hassan[17], R. Hauser[110], C.M. Hawkes[21], R.J. Hawkings[37], Y. Hayashi[157], D. Hayden[110], C. Hayes[109], R.L. Hayes[118], C.P. Hays[130], J.M. Hays[97], H.S. Hayward[95], F. He[64a], M. He[14,115c], Y. He[50], Y. He[99], N.B. Heatley[97], V. Hedberg[101], A.L. Heggelund[129], N.D. Hehir[97,*], C. Heidegger[56], K.K. Heidegger[56], J. Heilman[35], S. Heim[50], T. Heim[18a], J.G. Heinlein[132], J.J. Heinrich[127], L. Heinrich[113,aa], J. Hejbal[135], A. Held[175], S. Hellesund[17], C.M. Helling[169], S. Hellman[49a,49b], R.C.W. Henderson[94], L. Henkelmann[33], A.M. Henriques Correia[37], H. Herde[101], Y. Hernández Jiménez[149], L.M. Herrmann[25], T. Herrmann[52], G. Herten[56], R. Hertenberger[112], L. Hervas[37], M.E. Hesping[103], N.P. Hessey[160a], J. Hessler[113], M. Hidaoui[36b], N. Hidic[137], E. Hill[159], S.J. Hillier[21], J.R. Hinds[110], F. Hinterkeuser[25], M. Hirose[128], S. Hirose[161], D. Hirschbuehl[176], T.G. Hitchings[104], B. Hiti[96], J. Hobbs[149], R. Hobincu[28e], N. Hod[174], M.C. Hodgkinson[143], B.H. Hodkinson[130], A. Hoecker[37], D.D. Hofer[109], J. Hofer[168], T. Holm[25], M. Holzbock[37], L.B.A.H. Hommels[33], B.P. Honan[104], J.J. Hong[70], J. Hong[64c], T.M. Hong[133], B.H. Hooberman[167], W.H. Hopkins[6], M.C. Hoppesch[167], Y. Horii[114], M.E. Horstmann[113], S. Hou[152], M.R. Housenga[167], A.S. Howard[96], J. Howarth[61], J. Hoya[6], M. Hrabovsky[126], A. Hrynevich[50], T. Hryn'ova[4], P.J. Hsu[67], S.-C. Hsu[142], T. Hsu[68], M. Hu[18a], Q. Hu[64a], S. Huang[33], X. Huang[14,115c], Y. Huang[143], Y. Huang[103], Y. Huang[14], Z. Huang[104], Z. Hubacek[136], M. Huebner[25], F. Huegging[25], T.B. Huffman[130], M. Hufnagel Maranha De Faria[85a], C.A. Hugli[50], M. Huhtinen[37], S.K. Huiberts[17], R. Hulsken[107], N. Huseynov[12,f], J. Huston[110], J. Huth[63], R. Hyneman[147], G. Iacobucci[58], G. Iakovidis[30], L. Iconomidou-Fayard[68], J.P. Iddon[37], P. Iengo[74a,74b], R. Iguchi[157], Y. Iiyama[157], T. Iizawa[130], Y. Ikegami[86], D. Iliadis[156], N. Ilic[159], H. Imam[85c], G. Inacio Goncalves[85d], T. Ingebretsen Carlson[49a,49b], J.M. Inglis[97], G. Introzzi[75a,75b], M. Iodice[79a], V. Ippolito[77a,77b], R.K. Irwin[95], M. Ishino[157], W. Islam[175], C. Issever[19], S. Istin[22a,ag], H. Ito[173], R. Iuppa[80a,80b], A. Ivina[174], J.M. Izen[47], V. Izzo[74a], P. Jacka[135], P. Jackson[1], C.S. Jagfeld[112], G. Jain[160a], P. Jain[50], K. Jakobs[56], T. Jakoubek[174], J. Jamieson[61], W. Jang[157], M. Javurkova[106], P. Jawahar[104], L. Jeanty[127], J. Jejelava[153a], P. Jenni[56,e], C.E. Jessiman[35], C. Jia[64b], H. Jia[169], J. Jia[149], X. Jia[14,115c], Z. Jia[115a], C. Jiang[54], S. Jiggins[50], J. Jimenez Pena[13], S. Jin[115a], A. Jinaru[28b], O. Jinnouchi[158], P. Johansson[143], K.A. Johns[7], J.W. Johnson[140], F.A. Jolly[50], D.M. Jones[150], E. Jones[50], K.S. Jones[8], P. Jones[33], R.W.L. Jones[94], T.J. Jones[95], H.L. Joos[57,37], R. Joshi[123], J. Jovicevic[16], X. Ju[18a], J.J. Junggeburth[37], T. Junkermann[65a], A. Juste Rozas[13,t], M.K. Juzek[89], S. Kabana[141e], A. Kaczmarska[89], M. Kado[113], H. Kagan[123], M. Kagan[147], A. Kahn[132], C. Kahra[103], T. Kaji[157], E. Kajomovitz[154], N. Kakati[174], I. Kalaitzidou[56], C.W. Kalderon[30], N.J. Kang[140], D. Kar[34g], K. Karava[130], M.J. Kareem[160b], E. Karentzos[25],

O. Karkout[118], S.N. Karpov[40], Z.M. Karpova[40], V. Kartvelishvili[94], A.N. Karyukhin[39], E. Kasimi[156], J. Katzy[50], S. Kaur[35], K. Kawade[144], M.P. Kawale[124], C. Kawamoto[90], T. Kawamoto[64a], E.F. Kay[37], F.I. Kaya[162], S. Kazakos[110], V.F. Kazanin[39], Y. Ke[149], J.M. Keaveney[34a], R. Keeler[170], G.V. Kehris[63], J.S. Keller[35], J.J. Kempster[150], O. Kepka[135], J. Kerr[160b], B.P. Kerridge[138], S. Kersten[176], B.P. Kerševan[96], L. Keszeghova[29a], S. Ketabchi Haghighat[159], R.A. Khan[133], A. Khanov[125], A.G. Kharlamov[39], T. Kharlamova[39], E.E. Khoda[142], M. Kholodenko[134a], T.J. Khoo[19], G. Khoriauli[171], J. Khubua[153b,*], Y.A.R. Khwaira[131], B. Kibirige[34g], D. Kim[6], D.W. Kim[49a,49b], Y.K. Kim[41], N. Kimura[99], M.K. Kingston[57], A. Kirchhoff[57], C. Kirfel[25], F. Kirfel[25], J. Kirk[138], A.E. Kiryunin[113], S. Kita[161], C. Kitsaki[10], O. Kivernyk[25], M. Klassen[162], C. Klein[35], L. Klein[171], M.H. Klein[46], S.B. Klein[58], U. Klein[95], A. Klimentov[30], T. Klioutchnikova[37], P. Kluit[118], S. Kluth[113], E. Kneringer[81], T.M. Knight[159], A. Knue[51], D. Kobylianskii[174], S.F. Koch[130], M. Kocian[147], P. Kodyš[137], D.M. Koeck[127], P.T. Koenig[25], T. Koffas[35], O. Kolay[52], I. Koletsou[4], T. Komarek[89], K. Köneke[57], A.X.Y. Kong[1], T. Kono[122], N. Konstantinidis[99], P. Kontaxakis[58], B. Konya[101], R. Kopeliansky[43], S. Koperny[88a], K. Korcyl[89], K. Kordas[156,d], A. Korn[99], S. Korn[57], I. Korolkov[13], N. Korotkova[39], B. Kortman[118], O. Kortner[113], S. Kortner[113], W.H. Kostecka[119], V.V. Kostyukhin[145], A. Kotsokechagia[37], A. Kotwal[53], A. Koulouris[37], A. Kourkoumeli-Charalampidi[75a,75b], C. Kourkoumelis[9], E. Kourlitis[113,aa], O. Kovanda[127], R. Kowalewski[170], W. Kozanecki[127], A.S. Kozhin[39], V.A. Kramarenko[39], G. Kramberger[96], P. Kramer[25], M.W. Krasny[131], A. Krasznahorkay[37], A.C. Kraus[119], J.W. Kraus[176], J.A. Kremer[50], T. Kresse[52], L. Kretschmann[176], J. Kretzschmar[95], K. Kreul[19], P. Krieger[159], K. Krizka[21], K. Kroeninger[51], H. Kroha[113], J. Kroll[135], J. Kroll[132], K.S. Krowpman[110], U. Kruchonak[40], H. Krüger[25], N. Krumnack[83], M.C. Kruse[53], O. Kuchinskaia[39], S. Kuday[3a], S. Kuehn[37], R. Kuesters[56], T. Kuhl[50], V. Kukhtin[40], Y. Kulchitsky[40], S. Kuleshov[141d,141b], M. Kumar[34g], N. Kumari[50], P. Kumari[160b], A. Kupco[135], T. Kupfer[51], A. Kupich[39], O. Kuprash[56], H. Kurashige[87], L.L. Kurchaninov[160a], O. Kurdysh[68], Y.A. Kurochkin[38], A. Kurova[39], M. Kuze[158], A.K. Kvam[106], J. Kvita[126], T. Kwan[107], N.G. Kyriacou[109], L.A.O. Laatu[105], C. Lacasta[168], F. Lacava[77a,77b], H. Lacker[19], D. Lacour[131], N.N. Lad[99], E. Ladygin[40], A. Lafarge[42], B. Laforge[131], T. Lagouri[177], F.Z. Lahbabi[36a], S. Lai[57], J.E. Lambert[170], S. Lammers[70], W. Lampl[7], C. Lampoudis[156,d], G. Lamprinoudis[103], A.N. Lancaster[119], E. Lançon[30], U. Landgraf[56], M.P.J. Landon[97], V.S. Lang[56], O.K.B. Langrekken[129], A.J. Lankford[163], F. Lanni[37], K. Lantzsch[25], A. Lanza[75a], M. Lanzac Berrocal[168], J.F. Laporte[139], T. Lari[73a], F. Lasagni Manghi[24b], M. Lassnig[37], V. Latonova[135], S.D. Lawlor[143], Z. Lawrence[104], R. Lazaridou[172], M. Lazzaroni[73a,73b], H.D.M. Le[110], E.M. Le Boulicaut[177], L.T. Le Pottier[18a], B. Leban[24b,24a], A. Lebedev[83], M. LeBlanc[104], F. Ledroit-Guillon[62], S.C. Lee[152], S. Lee[49a,49b], T.F. Lee[95], L.L. Leeuw[34c], M. Lefebvre[170], C. Leggett[18a], G. Lehmann Miotto[37], M. Leigh[58], W.A. Leight[106], W. Leinonen[117], A. Leisos[156,r], M.A.L. Leite[85c], C.E. Leitgeb[19], R. Leitner[137], K.J.C. Leney[46], T. Lenz[25], S. Leone[76a], C. Leonidopoulos[54], A. Leopold[148], R. Les[110], C.G. Lester[33], M. Levchenko[39], J. Levêque[4], L.J. Levinson[174], G. Levrini[24b,24a], M.P. Lewicki[89], C. Lewis[142], D.J. Lewis[4], L. Lewitt[143], A. Li[30], B. Li[64b], C. Li[64a], C-Q. Li[113], H. Li[64a], H. Li[64b], H. Li[115a], H. Li[15], H. Li[64b], J. Li[64c], K. Li[14], L. Li[64c], M. Li[14,115c], S. Li[14,115c], S. Li[64d,64c], T. Li[5], X. Li[107], Z. Li[157], Z. Li[14,115c], Z. Li[64a], S. Liang[14,115c], Z. Liang[14], M. Liberatore[139], B. Liberti[78a], K. Lie[66c], J. Lieber Marin[85e], H. Lien[70], H. Lin[109], K. Lin[110], L. Linden[112], R.E. Lindley[7], J.H. Lindon[2], J. Ling[63], E. Lipeles[132], A. Lipniacka[17], A. Lister[169], J.D. Little[70], B. Liu[14], B.X. Liu[115b], D. Liu[64d,64c],

E.H.L. Liu [21], J.B. Liu [64a], J.K.K. Liu [33], K. Liu [64d], K. Liu [64d,64c], M. Liu [64a], M.Y. Liu [64a], P. Liu [14], Q. Liu [64d,142,64c], X. Liu [64a], X. Liu [64b], Y. Liu [115b,115c], Y.L. Liu [64b], Y.W. Liu [64a], S.L. Lloyd [97], E.M. Lobodzinska [50], P. Loch [7], E. Lodhi [159], T. Lohse [19], K. Lohwasser [143], E. Loiacono [50], J.D. Lomas [21], J.D. Long [43], I. Longarini [163], R. Longo [167], I. Lopez Paz [69], A. Lopez Solis [50], N.A. Lopez-canelas [7], N. Lorenzo Martinez [4], A.M. Lory [112], M. Losada [120a], G. Löschcke Centeno [150], O. Loseva [39], X. Lou [49a,49b], X. Lou [14,115c], A. Lounis [68], P.A. Love [94], G. Lu [14,115c], M. Lu [68], S. Lu [132], Y.J. Lu [152], H.J. Lubatti [142], C. Luci [77a,77b], F.L. Lucio Alves [115a], F. Luehring [70], O. Lukianchuk [68], B.S. Lunday [132], O. Lundberg [148], B. Lund-Jensen [148,*], N.A. Luongo [6], M.S. Lutz [37], A.B. Lux [26], D. Lynn [30], R. Lysak [135], E. Lytken [101], V. Lyubushkin [40], T. Lyubushkina [40], M.M. Lyukova [149], M.Firdaus M. Soberi [54], H. Ma [30], K. Ma [64a], L.L. Ma [64b], W. Ma [64a], Y. Ma [125], J.C. MacDonald [103], P.C. Machado De Abreu Farias [85e], R. Madar [42], T. Madula [99], J. Maeda [87], T. Maeno [30], P.T. Mafa [34c], H. Maguire [143], V. Maiboroda [139], A. Maio [134a,134b,134d], K. Maj [88a], O. Majersky [50], S. Majewski [127], N. Makovec [68], V. Maksimovic [16], B. Malaescu [131], Pa. Malecki [89], V.P. Maleev [39], F. Malek [62,m], M. Mali [96], D. Malito [98], U. Mallik [82,*], S. Maltezos[10], S. Malyukov[40], J. Mamuzic [13], G. Mancini [55], M.N. Mancini [27], G. Manco [75a,75b], J.P. Mandalia [97], S.S. Mandarry [150], I. Mandić [96], L. Manhaes de Andrade Filho [85a], I.M. Maniatis [174], J. Manjarres Ramos [92], D.C. Mankad [174], A. Mann [112], S. Manzoni [37], L. Mao [64c], X. Mapekula [34c], A. Marantis [156,r], G. Marchiori [5], M. Marcisovsky [135], C. Marcon [73a], M. Marinescu [21], S. Marium [50], M. Marjanovic [124], A. Markhoos [56], M. Markovitch [68], M.K. Maroun [106], E.J. Marshall [94], Z. Marshall [18a], S. Marti-Garcia [168], J. Martin [99], T.A. Martin [138], V.J. Martin [54], B. Martin dit Latour [17], L. Martinelli [77a,77b], M. Martinez [13,t], P. Martinez Agullo [168], V.I. Martinez Outschoorn [106], P. Martinez Suarez [13], S. Martin-Haugh [138], G. Martinovicova [137], V.S. Martoiu [28b], A.C. Martyniuk [99], A. Marzin [37], D. Mascione [80a,80b], L. Masetti [103], J. Masik [104], A.L. Maslennikov [39], S.L. Mason [43], P. Massarotti [74a,74b], P. Mastrandrea [76a,76b], A. Mastroberardino [45b,45a], T. Masubuchi [128], T.T. Mathew [127], T. Mathisen [166], J. Matousek [137], D.M. Mattern [51], J. Maurer [28b], T. Maurin [61], A.J. Maury [68], B. Maček [96], D.A. Maximov [39], A.E. May [104], R. Mazini [34g], I. Maznas [119], M. Mazza [110], S.M. Mazza [140], E. Mazzeo [73a,73b], J.P. Mc Gowan [170], S.P. Mc Kee [109], C.A. Mc Lean [6], C.C. McCracken [169], E.F. McDonald [108], A.E. McDougall [118], L.F. Mcelhinney [94], J.A. Mcfayden [150], R.P. McGovern [132], R.P. Mckenzie [34g], T.C. Mclachlan [50], D.J. Mclaughlin [99], S.J. McMahon [138], C.M. Mcpartland [95], R.A. McPherson [170,x], S. Mehlhase [112], A. Mehta [95], D. Melini [168], B.R. Mellado Garcia [34g], A.H. Melo [57], F. Meloni [50], A.M. Mendes Jacques Da Costa [104], H.Y. Meng [159], L. Meng [94], S. Menke [113], M. Mentink [37], E. Meoni [45b,45a], G. Mercado [119], S. Merianos [156], C. Merlassino [71a,71c], L. Merola [74a,74b], C. Meroni [73a,73b], J. Metcalfe [6], A.S. Mete [6], E. Meuser [103], C. Meyer [70], J-P. Meyer [139], R.P. Middleton [138], L. Mijović [54], G. Mikenberg [174], M. Mikestikova [135], M. Mikuž [96], H. Mildner [103], A. Milic [37], D.W. Miller [41], E.H. Miller [147], L.S. Miller [35], A. Milov [174], D.A. Milstead[49a,49b], T. Min[115a], A.A. Minaenko [39], I.A. Minashvili [153b], A.I. Mincer [121], B. Mindur [88a], M. Mineev [40], Y. Mino [90], L.M. Mir [13], M. Miralles Lopez [61], M. Mironova [18a], M.C. Missio [117], A. Mitra [172], V.A. Mitsou [168], Y. Mitsumori [114], O. Miu [159], P.S. Miyagawa [97], T. Mkrtchyan [65a], M. Mlinarevic [99], T. Mlinarevic [99], M. Mlynarikova [37], S. Mobius [20], P. Mogg [112], M.H. Mohamed Farook [116], A.F. Mohammed [14,115c], S. Mohapatra [43], G. Mokgatitswane [34g], L. Moleri [174], B. Mondal [145], S. Mondal [136], K. Mönig [50], E. Monnier [105], L. Monsonis Romero[168], J. Montejo Berlingen [13], A. Montella [49a,49b], M. Montella [123], F. Montereali [79a,79b], F. Monticelli [93], S. Monzani [71a,71c], A. Morancho Tarda [44], N. Morange [68], A.L. Moreira De Carvalho [50], M. Moreno Llácer [168], C. Moreno Martinez [58],

J.M. Moreno Perez[23b], P. Morettini[59b], S. Morgenstern[37], M. Morii[63], M. Morinaga[157], M. Moritsu[91], F. Morodei[77a,77b], P. Moschovakos[37], B. Moser[130], M. Mosidze[153b], T. Moskalets[46], P. Moskvitina[117], J. Moss[32,j], P. Moszkowicz[88a], A. Moussa[36d], Y. Moyal[174], E.J.W. Moyse[106], O. Mtintsilana[34g], S. Muanza[105], J. Mueller[133], D. Muenstermann[94], R. Müller[37], G.A. Mullier[166], A.J. Mullin[33], J.J. Mullin[132], A.E. Mulski[63], D.P. Mungo[159], D. Munoz Perez[168], F.J. Munoz Sanchez[104], M. Murin[104], W.J. Murray[172,138], M. Muškinja[96], C. Mwewa[30], A.G. Myagkov[39,a], A.J. Myers[8], G. Myers[109], M. Myska[136], B.P. Nachman[18a], K. Nagai[130], K. Nagano[86], R. Nagasaka[157], J.L. Nagle[30,ae], E. Nagy[105], A.M. Nairz[37], Y. Nakahama[86], K. Nakamura[86], K. Nakkalil[5], H. Nanjo[128], E.A. Narayanan[46], Y. Narukawa[157], I. Naryshkin[39], L. Nasella[73a,73b], S. Nasri[120b], C. Nass[25], G. Navarro[23a], J. Navarro-Gonzalez[168], A. Nayaz[19], P.Y. Nechaeva[39], S. Nechaeva[24b,24a], F. Nechansky[135], L. Nedic[130], T.J. Neep[21], A. Negri[75a,75b], M. Negrini[24b], C. Nellist[118], C. Nelson[107], K. Nelson[109], S. Nemecek[135], M. Nessi[37,g], M.S. Neubauer[167], F. Neuhaus[103], J. Neundorf[50], J. Newell[95], P.R. Newman[21], C.W. Ng[133], Y.W.Y. Ng[50], B. Ngair[120a], H.D.N. Nguyen[111], R.B. Nickerson[130], R. Nicolaidou[139], J. Nielsen[140], M. Niemeyer[57], J. Niermann[37], N. Nikiforou[37], V. Nikolaenko[39,a], I. Nikolic-Audit[131], K. Nikolopoulos[21], P. Nilsson[30], I. Ninca[50], G. Ninio[155], A. Nisati[77a], N. Nishu[2], R. Nisius[113], N. Nitika[71a,71c], J-E. Nitschke[52], E.K. Nkadimeng[34g], T. Nobe[157], T. Nommensen[151], M.B. Norfolk[143], B.J. Norman[35], M. Noury[36a], J. Novak[96], T. Novak[96], L. Novotny[136], R. Novotny[116], L. Nozka[126], K. Ntekas[163], N.M.J. Nunes De Moura Junior[85b], J. Ocariz[131], A. Ochi[87], I. Ochoa[134a], S. Oerdek[50,u], J.T. Offermann[41], A. Ogrodnik[137], A. Oh[104], C.C. Ohm[148], H. Oide[86], R. Oishi[157], M.L. Ojeda[37], Y. Okumura[157], L.F. Oleiro Seabra[134a], I. Oleksiyuk[58], S.A. Olivares Pino[141d], G. Oliveira Correa[13], D. Oliveira Damazio[30], J.L. Oliver[163], Ö.O. Öncel[56], A.P. O'Neill[20], A. Onofre[134a,134e], P.U.E. Onyisi[11], M.J. Oreglia[41], D. Orestano[79a,79b], N. Orlando[13], R.S. Orr[159], L.M. Osojnak[132], Y. Osumi[114], G. Otero y Garzon[31], H. Otono[91], P.S. Ott[65a], G.J. Ottino[18a], M. Ouchrif[36d], F. Ould-Saada[129], T. Ovsiannikova[142], M. Owen[61], R.E. Owen[138], V.E. Ozcan[22a], F. Ozturk[89], N. Ozturk[8], S. Ozturk[84], H.A. Pacey[130], A. Pacheco Pages[13], C. Padilla Aranda[13], G. Padovano[77a,77b], S. Pagan Griso[18a], G. Palacino[70], A. Palazzo[72a,72b], J. Pampel[25], J. Pan[177], T. Pan[66a], D.K. Panchal[11], C.E. Pandini[118], J.G. Panduro Vazquez[138], H.D. Pandya[1], H. Pang[15], P. Pani[50], G. Panizzo[71a,71c], L. Panwar[131], L. Paolozzi[58], S. Parajuli[167], A. Paramonov[6], C. Paraskevopoulos[55], D. Paredes Hernandez[66b], A. Pareti[75a,75b], K.R. Park[43], T.H. Park[159], M.A. Parker[33], F. Parodi[59b,59a], V.A. Parrish[54], J.A. Parsons[43], U. Parzefall[56], B. Pascual Dias[111], L. Pascual Dominguez[102], E. Pasqualucci[77a], S. Passaggio[59b], F. Pastore[98], P. Patel[89], U.M. Patel[53], J.R. Pater[104], T. Pauly[37], F. Pauwels[137], C.I. Pazos[162], M. Pedersen[129], R. Pedro[134a], S.V. Peleganchuk[39], O. Penc[37], E.A. Pender[54], S. Peng[15], G.D. Penn[177], K.E. Penski[112], M. Penzin[39], B.S. Peralva[85d], A.P. Pereira Peixoto[142], L. Pereira Sanchez[147], D.V. Perepelitsa[30,ae], G. Perera[106], E. Perez Codina[160a], M. Perganti[10], H. Pernegger[37], S. Perrella[77a,77b], O. Perrin[42], K. Peters[50], R.F.Y. Peters[104], B.A. Petersen[37], T.C. Petersen[44], E. Petit[105], V. Petousis[136], C. Petridou[156,d], T. Petru[137], A. Petrukhin[145], M. Pettee[18a], A. Petukhov[84], K. Petukhova[37], R. Pezoa[141f], L. Pezzotti[37], G. Pezzullo[177], A.J. Pfleger[37], T.M. Pham[175], T. Pham[108], P.W. Phillips[138], G. Piacquadio[149], E. Pianori[18a], F. Piazza[127], R. Piegaia[31], D. Pietreanu[28b], A.D. Pilkington[104], M. Pinamonti[71a,71c], J.L. Pinfold[2], B.C. Pinheiro Pereira[134a], J. Pinol Bel[13], A.E. Pinto Pinoargote[139,139], L. Pintucci[71a,71c], K.M. Piper[150], A. Pirttikoski[58], D.A. Pizzi[35], L. Pizzimento[66b], A. Pizzini[118], M.-A. Pleier[30], V. Pleskot[137], E. Plotnikova[40], G. Poddar[97], R. Poettgen[101],

L. Poggioli [131], S. Polacek [137], G. Polesello [75a], A. Poley [146,160a], A. Polini [24b], C.S. Pollard [172], Z.B. Pollock [123], E. Pompa Pacchi [124], N.I. Pond [99], D. Ponomarenko [70], L. Pontecorvo [37], S. Popa [28a], G.A. Popeneciu [28d], A. Poreba [37], D.M. Portillo Quintero [160a], S. Pospisil [136], M.A. Postill [143], P. Postolache [28c], K. Potamianos [172], P.A. Potepa [88a], I.N. Potrap [40], C.J. Potter [33], H. Potti [151], J. Poveda [168], M.E. Pozo Astigarraga [37], A. Prades Ibanez [78a,78b], J. Pretel [170], D. Price [104], M. Primavera [72a], L. Primomo [71a,71c], M.A. Principe Martin [102], R. Privara [126], T. Procter [61], M.L. Proffitt [142], N. Proklova [132], K. Prokofiev [66c], G. Proto [113], J. Proudfoot [6], M. Przybycien [88a], W.W. Przygoda [88b], A. Psallidas [48], J.E. Puddefoot [143], D. Pudzha [56], D. Pyatiizbyantseva [39], J. Qian [109], R. Qian [110], D. Qichen [104], Y. Qin [13], T. Qiu [54], A. Quadt [57], M. Queitsch-Maitland [104], G. Quetant [58], R.P. Quinn [169], G. Rabanal Bolanos [63], D. Rafanoharana [56], F. Raffaeli [78a,78b], F. Ragusa [73a,73b], J.L. Rainbolt [41], J.A. Raine [58], S. Rajagopalan [30], E. Ramakoti [39], L. Rambelli [59b,59a], I.A. Ramirez-Berend [35], K. Ran [50,115c], D.S. Rankin [132], N.P. Rapheeha [34g], H. Rasheed [28b], V. Raskina [131], D.F. Rassloff [65a], A. Rastogi [18a], S. Rave [103], S. Ravera [59b,59a], B. Ravina [57], I. Ravinovich [174], M. Raymond [37], A.L. Read [129], N.P. Readioff [143], D.M. Rebuzzi [75a,75b], G. Redlinger [30], A.S. Reed [113], K. Reeves [27], J.A. Reidelsturz [176], D. Reikher [127], A. Rej [51], C. Rembser [37], M. Renda [28b], F. Renner [50], A.G. Rennie [163], A.L. Rescia [50], S. Resconi [73a], M. Ressegotti [59b,59a], S. Rettie [37], J.G. Reyes Rivera [110], E. Reynolds [18a], O.L. Rezanova [39], P. Reznicek [137], H. Riani [36d], N. Ribaric [53], E. Ricci [80a,80b], R. Richter [113], S. Richter [49a,49b], E. Richter-Was [88b], M. Ridel [131], S. Ridouani [36d], P. Rieck [121], P. Riedler [37], E.M. Riefel [49a,49b], J.O. Rieger [118], M. Rijssenbeek [149], M. Rimoldi [37], L. Rinaldi [24b,24a], P. Rincke [57,166], T.T. Rinn [30], M.P. Rinnagel [112], G. Ripellino [166], I. Riu [13], J.C. Rivera Vergara [170], F. Rizatdinova [125], E. Rizvi [97], B.R. Roberts [18a], S.S. Roberts [140], S.H. Robertson [107,x], D. Robinson [33], M. Robles Manzano [103], A. Robson [61], A. Rocchi [78a,78b], C. Roda [76a,76b], S. Rodriguez Bosca [37], Y. Rodriguez Garcia [23a], A.M. Rodríguez Vera [119], S. Roe [37], J.T. Roemer [37], O. Røhne [129], R.A. Rojas [106], C.P.A. Roland [131], J. Roloff [30], A. Romaniouk [81], E. Romano [75a,75b], M. Romano [24b], A.C. Romero Hernandez [167], N. Rompotis [95], L. Roos [131], S. Rosati [77a], B.J. Rosser [41], E. Rossi [130], E. Rossi [74a,74b], L.P. Rossi [63], L. Rossini [56], R. Rosten [123], M. Rotaru [28b], B. Rottler [56], C. Rougier [92], D. Rousseau [68], D. Rousso [50], A. Roy [167], S. Roy-Garand [159], A. Rozanov [105], Z.M.A. Rozario [61], Y. Rozen [154], A. Rubio Jimenez [168], V.H. Ruelas Rivera [19], T.A. Ruggeri [1], A. Ruggiero [130], A. Ruiz-Martinez [168], A. Rummler [37], Z. Rurikova [56], N.A. Rusakovich [40], H.L. Russell [170], G. Russo [77a,77b], J.P. Rutherfoord [7], S. Rutherford Colmenares [33], M. Rybar [137], E.B. Rye [129], A. Ryzhov [46], J.A. Sabater Iglesias [58], H.F-W. Sadrozinski [140], F. Safai Tehrani [77a], B. Safarzadeh Samani [138], S. Saha [1], M. Sahinsoy [84], A. Saibel [168], M. Saimpert [139], M. Saito [157], T. Saito [157], A. Sala [73a,73b], D. Salamani [37], A. Salnikov [147], J. Salt [168], A. Salvador Salas [155], D. Salvatore [45b,45a], F. Salvatore [150], A. Salzburger [37], D. Sammel [56], E. Sampson [94], D. Sampsonidis [156,d], D. Sampsonidou [127], J. Sánchez [168], V. Sanchez Sebastian [168], H. Sandaker [129], C.O. Sander [50], J.A. Sandesara [106], M. Sandhoff [176], C. Sandoval [23b], L. Sanfilippo [65a], D.P.C. Sankey [138], T. Sano [90], A. Sansoni [55], L. Santi [37,77b], C. Santoni [42], H. Santos [134a,134b], A. Santra [174], E. Sanzani [24b,24a], K.A. Saoucha [165], J.G. Saraiva [134a,134d], J. Sardain [7], O. Sasaki [86], K. Sato [161], C. Sauer [37], E. Sauvan [4], P. Savard [159,ac], R. Sawada [157], C. Sawyer [138], L. Sawyer [100], C. Sbarra [24b], A. Sbrizzi [24b,24a], T. Scanlon [99], J. Schaarschmidt [142], U. Schäfer [103], A.C. Schaffer [68,46], D. Schaile [112], R.D. Schamberger [149], C. Scharf [19], M.M. Schefer [20], V.A. Schegelsky [39], D. Scheirich [137], M. Schernau [141e], C. Scheulen [58], C. Schiavi [59b,59a], M. Schioppa [45b,45a], B. Schlag [147,l], S. Schlenker [37], J. Schmeing [176], M.A. Schmidt [176], K. Schmieden [103], C. Schmitt [103],

N. Schmitt[103], S. Schmitt[50], L. Schoeffel[139], A. Schoening[65b], P.G. Scholer[35], E. Schopf[130], M. Schott[25], J. Schovancova[37], S. Schramm[58], T. Schroer[58], H-C. Schultz-Coulon[65a], M. Schumacher[56], B.A. Schumm[140], Ph. Schune[139], A.J. Schuy[142], H.R. Schwartz[140], A. Schwartzman[147], T.A. Schwarz[109], Ph. Schwemling[139], R. Schwienhorst[110], F.G. Sciacca[20], A. Sciandra[30], G. Sciolla[27], F. Scuri[76a], C.D. Sebastiani[95], K. Sedlaczek[119], S.C. Seidel[116], A. Seiden[140], B.D. Seidlitz[43], C. Seitz[50], J.M. Seixas[85b], G. Sekhniaidze[74a], L. Selem[62], N. Semprini-Cesari[24b,24a], A. Semushin[178,39], D. Sengupta[58], V. Senthilkumar[168], L. Serin[68], M. Sessa[78a,78b], H. Severini[124], F. Sforza[59b,59a], A. Sfyrla[58], Q. Sha[14], E. Shabalina[57], A.H. Shah[33], R. Shaheen[148], J.D. Shahinian[132], D. Shaked Renous[174], L.Y. Shan[14], M. Shapiro[18a], A. Sharma[37], A.S. Sharma[169], P. Sharma[30], P.B. Shatalov[39], K. Shaw[150], S.M. Shaw[104], Q. Shen[64c], D.J. Sheppard[146], P. Sherwood[99], L. Shi[99], X. Shi[14], S. Shimizu[86], C.O. Shimmin[177], I.P.J. Shipsey[130], S. Shirabe[91], M. Shiyakova[40,v], M.J. Shochet[41], D.R. Shope[129], B. Shrestha[124], S. Shrestha[123,af], I. Shreyber[39], M.J. Shroff[170], P. Sicho[135], A.M. Sickles[167], E. Sideras Haddad[34g,164], A.C. Sidley[118], A. Sidoti[24b], F. Siegert[52], Dj. Sijacki[16], F. Sili[93], J.M. Silva[54], I. Silva Ferreira[85b], M.V. Silva Oliveira[30], S.B. Silverstein[49a], S. Simion[68], R. Simoniello[37], E.L. Simpson[104], H. Simpson[150], L.R. Simpson[109], S. Simsek[84], S. Sindhu[57], P. Sinervo[159], S. Singh[30], S. Sinha[50], S. Sinha[104], M. Sioli[24b,24a], I. Siral[37], E. Sitnikova[50], J. Sjölin[49a,49b], A. Skaf[57], E. Skorda[21], P. Skubic[124], M. Slawinska[89], I. Slazyk[17], V. Smakhtin[174], B.H. Smart[138], S.Yu. Smirnov[39], Y. Smirnov[39], L.N. Smirnova[39,a], O. Smirnova[101], A.C. Smith[43], D.R. Smith[163], E.A. Smith[41], J.L. Smith[104], R. Smith[147], H. Smitmanns[103], M. Smizanska[94], K. Smolek[136], A.A. Snesarev[39], H.L. Snoek[118], S. Snyder[30], R. Sobie[170,x], A. Soffer[155], C.A. Solans Sanchez[37], E.Yu. Soldatov[39], U. Soldevila[168], A.A. Solodkov[39], S. Solomon[27], A. Soloshenko[40], K. Solovieva[56], O.V. Solovyanov[42], P. Sommer[52], A. Sonay[13], W.Y. Song[160b], A. Sopczak[136], A.L. Sopio[54], F. Sopkova[29b], J.D. Sorenson[116], I.R. Sotarriva Alvarez[158], V. Sothilingam[65a], O.J. Soto Sandoval[141c,141b], S. Sottocornola[70], R. Soualah[165], Z. Soumaimi[36e], D. South[50], N. Soybelman[174], S. Spagnolo[72a,72b], M. Spalla[113], D. Sperlich[56], G. Spigo[37], B. Spisso[74a,74b], D.P. Spiteri[61], M. Spousta[137], E.J. Staats[35], R. Stamen[65a], A. Stampekis[21], E. Stanecka[89], W. Stanek-Maslouska[50], M.V. Stange[52], B. Stanislaus[18a], M.M. Stanitzki[50], B. Stapf[50], E.A. Starchenko[39], G.H. Stark[140], J. Stark[92], P. Staroba[135], P. Starovoitov[65a], S. Stärz[107], R. Staszewski[89], G. Stavropoulos[48], A. Stefl[37], P. Steinberg[30], B. Stelzer[146,160a], H.J. Stelzer[133], O. Stelzer-Chilton[160a], H. Stenzel[60], T.J. Stevenson[150], G.A. Stewart[37], J.R. Stewart[125], M.C. Stockton[37], G. Stoicea[28b], M. Stolarski[134a], S. Stonjek[113], A. Straessner[52], J. Strandberg[148], S. Strandberg[49a,49b], M. Stratmann[176], M. Strauss[124], T. Strebler[105], P. Strizenec[29b], R. Ströhmer[171], D.M. Strom[127], R. Stroynowski[46], A. Strubig[49a,49b], S.A. Stucci[30], B. Stugu[17], J. Stupak[124], N.A. Styles[50], D. Su[147], S. Su[64a], W. Su[64d], X. Su[64a], D. Suchy[29a], K. Sugizaki[157], V.V. Sulin[39], M.J. Sullivan[95], D.M.S. Sultan[130], L. Sultanaliyeva[39], S. Sultansoy[3b], T. Sumida[90], S. Sun[175], W. Sun[14], O. Sunneborn Gudnadottir[166], N. Sur[105], M.R. Sutton[150], H. Suzuki[161], M. Svatos[135], M. Swiatlowski[160a], T. Swirski[171], I. Sykora[29a], M. Sykora[137], T. Sykora[137], D. Ta[103], K. Tackmann[50,u], A. Taffard[163], R. Tafirout[160a], J.S. Tafoya Vargas[68], Y. Takubo[86], M. Talby[105], A.A. Talyshev[39], K.C. Tam[66b], N.M. Tamir[155], A. Tanaka[157], J. Tanaka[157], R. Tanaka[68], M. Tanasini[149], Z. Tao[169], S. Tapia Araya[141f], S. Tapprogge[103], A. Tarek Abouelfadl Mohamed[110], S. Tarem[154], K. Tariq[14], G. Tarna[28b], G.F. Tartarelli[73a], M.J. Tartarin[92], P. Tas[137], M. Tasevsky[135], E. Tassi[45b,45a], A.C. Tate[167], G. Tateno[157], Y. Tayalati[36e,w], G.N. Taylor[108], W. Taylor[160b], P. Teixeira-Dias[98], J.J. Teoh[159],

K. Terashi[157], J. Terron[102], S. Terzo[13], M. Testa[55], R.J. Teuscher[159,x], A. Thaler[81], O. Theiner[58], T. Theveneaux-Pelzer[105], O. Thielmann[176], D.W. Thomas[98], J.P. Thomas[21], E.A. Thompson[18a], P.D. Thompson[21], E. Thomson[132], R.E. Thornberry[46], C. Tian[64a], Y. Tian[58], V. Tikhomirov[39,a], Yu.A. Tikhonov[39], S. Timoshenko[39], D. Timoshyn[137], E.X.L. Ting[1], P. Tipton[177], A. Tishelman-Charny[30], S.H. Tlou[34g], K. Todome[158], S. Todorova-Nova[137], S. Todt[52], L. Toffolin[71a,71c], M. Togawa[86], J. Tojo[91], S. Tokár[29a], K. Tokushuku[86], O. Toldaiev[70], G. Tolkachev[105], M. Tomoto[86,114], L. Tompkins[147,l], E. Torrence[127], H. Torres[92], E. Torró Pastor[168], M. Toscani[31], C. Tosciri[41], M. Tost[11], D.R. Tovey[143], I.S. Trandafir[28b], T. Trefzger[171], A. Tricoli[30], I.M. Trigger[160a], S. Trincaz-Duvoid[131], D.A. Trischuk[27], B. Trocmé[62], A. Tropina[40], L. Truong[34c], M. Trzebinski[89], A. Trzupek[89], F. Tsai[149], M. Tsai[109], A. Tsiamis[156], P.V. Tsiareshka[40], S. Tsigaridas[160a], A. Tsirigotis[156,r], V. Tsiskaridze[159], E.G. Tskhadadze[153a], M. Tsopoulou[156], Y. Tsujikawa[90], I.I. Tsukerman[39], V. Tsulaia[18a], S. Tsuno[86], K. Tsuri[122], D. Tsybychev[149], Y. Tu[66b], A. Tudorache[28b], V. Tudorache[28b], A.N. Tuna[63], S. Turchikhin[59b,59a], I. Turk Cakir[3a], R. Turra[73a], T. Turtuvshin[40], P.M. Tuts[43], S. Tzamarias[156,d], E. Tzovara[103], F. Ukegawa[161], P.A. Ulloa Poblete[141c,141b], E.N. Umaka[30], G. Unal[37], A. Undrus[30], G. Unel[163], J. Urban[29b], P. Urrejola[141a], G. Usai[8], R. Ushioda[158], M. Usman[111], F. Ustuner[54], Z. Uysal[84], V. Vacek[136], B. Vachon[107], T. Vafeiadis[37], A. Vaitkus[99], C. Valderanis[112], E. Valdes Santurio[49a,49b], M. Valente[160a], S. Valentinetti[24b,24a], A. Valero[168], E. Valiente Moreno[168], A. Vallier[92], J.A. Valls Ferrer[168], D.R. Van Arneman[118], T.R. Van Daalen[142], A. Van Der Graaf[51], P. Van Gemmeren[6], M. Van Rijnbach[37], S. Van Stroud[99], I. Van Vulpen[118], P. Vana[137], M. Vanadia[78a,78b], U.M. Vande Voorde[148], W. Vandelli[37], E.R. Vandewall[125], D. Vannicola[155], L. Vannoli[55], R. Vari[77a], E.W. Varnes[7], C. Varni[18b], D. Varouchas[68], L. Varriale[168], K.E. Varvell[151], M.E. Vasile[28b], L. Vaslin[86], A. Vasyukov[40], L.M. Vaughan[125], R. Vavricka[103], T. Vazquez Schroeder[37], J. Veatch[32], V. Vecchio[104], M.J. Veen[106], I. Veliscek[30], L.M. Veloce[159], F. Veloso[134a,134c], S. Veneziano[77a], A. Ventura[72a,72b], S. Ventura Gonzalez[139], A. Verbytskyi[113], M. Verducci[76a,76b], C. Vergis[97], M. Verissimo De Araujo[85b], W. Verkerke[118], J.C. Vermeulen[118], C. Vernieri[147], M. Vessella[163], M.C. Vetterli[146,ac], A. Vgenopoulos[103], N. Viaux Maira[141f], T. Vickey[143], O.E. Vickey Boeriu[143], G.H.A. Viehhauser[130], L. Vigani[65b], M. Vigl[113], M. Villa[24b,24a], M. Villaplana Perez[168], E.M. Villhauer[54], E. Vilucchi[55], M.G. Vincter[35], A. Visibile[118], C. Vittori[37], I. Vivarelli[24b,24a], E. Voevodina[113], F. Vogel[112], J.C. Voigt[52], P. Vokac[136], Yu. Volkotrub[88b], E. Von Toerne[25], A. Vorlander[176], B. Vormwald[37], V. Vorobel[137], K. Vorobev[39], M. Vos[168], K. Voss[145], M. Vozak[118], L. Vozdecky[124], N. Vranjes[16], M. Vranjes Milosavljevic[16], M. Vreeswijk[118], N.K. Vu[64d], R. Vuillermet[37], O. Vujinovic[103], I. Vukotic[41], I.K. Vyas[35], S. Wada[161], C. Wagner[147], J.M. Wagner[18a], W. Wagner[176], S. Wahdan[176], H. Wahlberg[93], C.H. Waits[124], J. Walder[138], R. Walker[112], W. Walkowiak[145], A. Wall[132], E.J. Wallin[101], T. Wamorkar[6], A.Z. Wang[140], C. Wang[103], C. Wang[11], H. Wang[18a], J. Wang[66c], P. Wang[104], P. Wang[99], R. Wang[63], R. Wang[6], S.M. Wang[152], S. Wang[14], T. Wang[64a], W.T. Wang[82], W. Wang[14], X. Wang[167], X. Wang[64c], Y. Wang[64d], Y. Wang[115a], Y. Wang[64a], Z. Wang[109], Z. Wang[64d,53,64c], Z. Wang[109], A. Warburton[107], R.J. Ward[21], N. Warrack[61], S. Waterhouse[98], A.T. Watson[21], H. Watson[54], M.F. Watson[21], E. Watton[61,138], G. Watts[142], B.M. Waugh[99], J.M. Webb[56], C. Weber[30], H.A. Weber[19], M.S. Weber[20], S.M. Weber[65a], C. Wei[64a], Y. Wei[56], A.R. Weidberg[130], E.J. Weik[121], J. Weingarten[51], C. Weiser[56], C.J. Wells[50], T. Wenaus[30], B. Wendland[51], T. Wengler[37], N.S. Wenke[113], N. Wermes[25], M. Wessels[65a], A.M. Wharton[94], A.S. White[63], A. White[8], M.J. White[1], D. Whiteson[163],

L. Wickremasinghe[128], W. Wiedenmann[175], M. Wielers[138], C. Wiglesworth[44], D.J. Wilbern[124], H.G. Wilkens[37], J.J.H. Wilkinson[33], D.M. Williams[43], H.H. Williams[132], S. Williams[33], S. Willocq[106], B.J. Wilson[104], D.J. Wilson[104], P.J. Windischhofer[41], F.I. Winkel[31], F. Winklmeier[127], B.T. Winter[56], J.K. Winter[104], M. Wittgen[147], M. Wobisch[100], T. Wojtkowski[62], Z. Wolffs[118], J. Wollrath[37], M.W. Wolter[89], H. Wolters[134a,134c], M.C. Wong[140], E.L. Woodward[43], S.D. Worm[50], B.K. Wosiek[89], K.W. Woźniak[89], S. Wozniewski[57], K. Wraight[61], C. Wu[21], M. Wu[115b], M. Wu[117], S.L. Wu[175], X. Wu[58], X. Wu[64a], Y. Wu[64a], Z. Wu[4], J. Wuerzinger[113,aa], T.R. Wyatt[104], B.M. Wynne[54], S. Xella[44], L. Xia[115a], M. Xia[15], M. Xie[64a], A. Xiong[127], J. Xiong[18a], D. Xu[14], H. Xu[64a], L. Xu[64a], R. Xu[132], T. Xu[109], Y. Xu[142], Z. Xu[54], Z. Xu[115a], B. Yabsley[151], S. Yacoob[34a], Y. Yamaguchi[86], E. Yamashita[157], H. Yamauchi[161], T. Yamazaki[18a], Y. Yamazaki[87], S. Yan[61], Z. Yan[106], H.J. Yang[64c,64d], H.T. Yang[64a], S. Yang[64a], T. Yang[66c], X. Yang[37], X. Yang[14], Y. Yang[46], Y. Yang[64a], W-M. Yao[18a], H. Ye[57], J. Ye[14], S. Ye[30], X. Ye[64a], Y. Yeh[99], I. Yeletskikh[40], B. Yeo[18b], M.R. Yexley[99], T.P. Yildirim[130], P. Yin[43], K. Yorita[173], S. Younas[28b], C.J.S. Young[37], C. Young[147], C. Yu[14,115c], Y. Yu[64a], J. Yuan[14,115c], M. Yuan[109], R. Yuan[64d,64c], L. Yue[99], M. Zaazoua[64a], B. Zabinski[89], I. Zahir[36a], E. Zaid[54], Z.K. Zak[89], T. Zakareishvili[168], S. Zambito[58], J.A. Zamora Saa[141d,141b], J. Zang[157], D. Zanzi[56], R. Zanzottera[73a,73b], O. Zaplatilek[136], C. Zeitnitz[176], H. Zeng[14], J.C. Zeng[167], D.T. Zenger Jr[27], O. Zenin[39], T. Ženiš[29a], S. Zenz[97], S. Zerradi[36a], D. Zerwas[68], M. Zhai[14,115c], D.F. Zhang[143], J. Zhang[64b], J. Zhang[6], K. Zhang[14,115c], L. Zhang[64a], L. Zhang[115a], P. Zhang[14,115c], R. Zhang[175], S. Zhang[109], S. Zhang[92], T. Zhang[157], X. Zhang[64c], Y. Zhang[142], Y. Zhang[99], Y. Zhang[115a], Z. Zhang[18a], Z. Zhang[64b], Z. Zhang[68], H. Zhao[142], T. Zhao[64b], Y. Zhao[140], Z. Zhao[64a], Z. Zhao[64a], A. Zhemchugov[40], J. Zheng[115a], K. Zheng[167], X. Zheng[64a], Z. Zheng[147], D. Zhong[167], B. Zhou[109], H. Zhou[7], N. Zhou[64c], Y. Zhou[15], Y. Zhou[115a], Y. Zhou[7], C.G. Zhu[64b], J. Zhu[109], X. Zhu[64d], Y. Zhu[64c], Y. Zhu[64a], X. Zhuang[14], K. Zhukov[70], N.I. Zimine[40], J. Zinsser[65b], M. Ziolkowski[145], L. Živković[16], A. Zoccoli[24b,24a], K. Zoch[63], T.G. Zorbas[143], O. Zormpa[48], W. Zou[43], L. Zwalinski[37].

[1]Department of Physics, University of Adelaide, Adelaide; Australia.
[2]Department of Physics, University of Alberta, Edmonton AB; Canada.
[3(a)]Department of Physics, Ankara University, Ankara;[(b)]Division of Physics, TOBB University of Economics and Technology, Ankara; Türkiye.
[4]LAPP, Université Savoie Mont Blanc, CNRS/IN2P3, Annecy; France.
[5]APC, Université Paris Cité, CNRS/IN2P3, Paris; France.
[6]High Energy Physics Division, Argonne National Laboratory, Argonne IL; United States of America.
[7]Department of Physics, University of Arizona, Tucson AZ; United States of America.
[8]Department of Physics, University of Texas at Arlington, Arlington TX; United States of America.
[9]Physics Department, National and Kapodistrian University of Athens, Athens; Greece.
[10]Physics Department, National Technical University of Athens, Zografou; Greece.
[11]Department of Physics, University of Texas at Austin, Austin TX; United States of America.
[12]Institute of Physics, Azerbaijan Academy of Sciences, Baku; Azerbaijan.
[13]Institut de Física d'Altes Energies (IFAE), Barcelona Institute of Science and Technology, Barcelona; Spain.
[14]Institute of High Energy Physics, Chinese Academy of Sciences, Beijing; China.
[15]Physics Department, Tsinghua University, Beijing; China.
[16]Institute of Physics, University of Belgrade, Belgrade; Serbia.

[17]Department for Physics and Technology, University of Bergen, Bergen; Norway.
[18](a)Physics Division, Lawrence Berkeley National Laboratory, Berkeley CA;(b)University of California, Berkeley CA; United States of America.
[19]Institut für Physik, Humboldt Universität zu Berlin, Berlin; Germany.
[20]Albert Einstein Center for Fundamental Physics and Laboratory for High Energy Physics, University of Bern, Bern; Switzerland.
[21]School of Physics and Astronomy, University of Birmingham, Birmingham; United Kingdom.
[22](a)Department of Physics, Bogazici University, Istanbul;(b)Department of Physics Engineering, Gaziantep University, Gaziantep;(c)Department of Physics, Istanbul University, Istanbul; Türkiye.
[23](a)Facultad de Ciencias y Centro de Investigaciónes, Universidad Antonio Nariño, Bogotá;(b)Departamento de Física, Universidad Nacional de Colombia, Bogotá; Colombia.
[24](a)Dipartimento di Fisica e Astronomia A. Righi, Università di Bologna, Bologna;(b)INFN Sezione di Bologna; Italy.
[25]Physikalisches Institut, Universität Bonn, Bonn; Germany.
[26]Department of Physics, Boston University, Boston MA; United States of America.
[27]Department of Physics, Brandeis University, Waltham MA; United States of America.
[28](a)Transilvania University of Brasov, Brasov;(b)Horia Hulubei National Institute of Physics and Nuclear Engineering, Bucharest;(c)Department of Physics, Alexandru Ioan Cuza University of Iasi, Iasi;(d)National Institute for Research and Development of Isotopic and Molecular Technologies, Physics Department, Cluj-Napoca;(e)National University of Science and Technology Politechnica, Bucharest;(f)West University in Timisoara, Timisoara;(g)Faculty of Physics, University of Bucharest, Bucharest; Romania.
[29](a)Faculty of Mathematics, Physics and Informatics, Comenius University, Bratislava;(b)Department of Subnuclear Physics, Institute of Experimental Physics of the Slovak Academy of Sciences, Kosice; Slovak Republic.
[30]Physics Department, Brookhaven National Laboratory, Upton NY; United States of America.
[31]Universidad de Buenos Aires, Facultad de Ciencias Exactas y Naturales, Departamento de Física, y CONICET, Instituto de Física de Buenos Aires (IFIBA), Buenos Aires; Argentina.
[32]California State University, CA; United States of America.
[33]Cavendish Laboratory, University of Cambridge, Cambridge; United Kingdom.
[34](a)Department of Physics, University of Cape Town, Cape Town;(b)iThemba Labs, Western Cape;(c)Department of Mechanical Engineering Science, University of Johannesburg, Johannesburg;(d)National Institute of Physics, University of the Philippines Diliman (Philippines);(e)University of South Africa, Department of Physics, Pretoria;(f)University of Zululand, KwaDlangezwa;(g)School of Physics, University of the Witwatersrand, Johannesburg; South Africa.
[35]Department of Physics, Carleton University, Ottawa ON; Canada.
[36](a)Faculté des Sciences Ain Chock, Université Hassan II de Casablanca;(b)Faculté des Sciences, Université Ibn-Tofail, Kénitra;(c)Faculté des Sciences Semlalia, Université Cadi Ayyad, LPHEA-Marrakech;(d)LPMR, Faculté des Sciences, Université Mohamed Premier, Oujda;(e)Faculté des sciences, Université Mohammed V, Rabat;(f)Institute of Applied Physics, Mohammed VI Polytechnic University, Ben Guerir; Morocco.
[37]CERN, Geneva; Switzerland.
[38]Affiliated with an institute formerly covered by a cooperation agreement with CERN.
[39]Affiliated with an institute covered by a cooperation agreement with CERN.
[40]Affiliated with an international laboratory covered by a cooperation agreement with CERN.
[41]Enrico Fermi Institute, University of Chicago, Chicago IL; United States of America.
[42]LPC, Université Clermont Auvergne, CNRS/IN2P3, Clermont-Ferrand; France.
[43]Nevis Laboratory, Columbia University, Irvington NY; United States of America.

[44]Niels Bohr Institute, University of Copenhagen, Copenhagen; Denmark.
[45(a)]Dipartimento di Fisica, Università della Calabria, Rende;[(b)]INFN Gruppo Collegato di Cosenza, Laboratori Nazionali di Frascati; Italy.
[46]Physics Department, Southern Methodist University, Dallas TX; United States of America.
[47]Physics Department, University of Texas at Dallas, Richardson TX; United States of America.
[48]National Centre for Scientific Research "Demokritos", Agia Paraskevi; Greece.
[49(a)]Department of Physics, Stockholm University;[(b)]Oskar Klein Centre, Stockholm; Sweden.
[50]Deutsches Elektronen-Synchrotron DESY, Hamburg and Zeuthen; Germany.
[51]Fakultät Physik , Technische Universität Dortmund, Dortmund; Germany.
[52]Institut für Kern- und Teilchenphysik, Technische Universität Dresden, Dresden; Germany.
[53]Department of Physics, Duke University, Durham NC; United States of America.
[54]SUPA - School of Physics and Astronomy, University of Edinburgh, Edinburgh; United Kingdom.
[55]INFN e Laboratori Nazionali di Frascati, Frascati; Italy.
[56]Physikalisches Institut, Albert-Ludwigs-Universität Freiburg, Freiburg; Germany.
[57]II. Physikalisches Institut, Georg-August-Universität Göttingen, Göttingen; Germany.
[58]Département de Physique Nucléaire et Corpusculaire, Université de Genève, Genève; Switzerland.
[59(a)]Dipartimento di Fisica, Università di Genova, Genova;[(b)]INFN Sezione di Genova; Italy.
[60]II. Physikalisches Institut, Justus-Liebig-Universität Giessen, Giessen; Germany.
[61]SUPA - School of Physics and Astronomy, University of Glasgow, Glasgow; United Kingdom.
[62]LPSC, Université Grenoble Alpes, CNRS/IN2P3, Grenoble INP, Grenoble; France.
[63]Laboratory for Particle Physics and Cosmology, Harvard University, Cambridge MA; United States of America.
[64(a)]Department of Modern Physics and State Key Laboratory of Particle Detection and Electronics, University of Science and Technology of China, Hefei;[(b)]Institute of Frontier and Interdisciplinary Science and Key Laboratory of Particle Physics and Particle Irradiation (MOE), Shandong University, Qingdao;[(c)]School of Physics and Astronomy, Shanghai Jiao Tong University, Key Laboratory for Particle Astrophysics and Cosmology (MOE), SKLPPC, Shanghai;[(d)]Tsung-Dao Lee Institute, Shanghai;[(e)]School of Physics and Microelectronics, Zhengzhou University; China.
[65(a)]Kirchhoff-Institut für Physik, Ruprecht-Karls-Universität Heidelberg, Heidelberg;[(b)]Physikalisches Institut, Ruprecht-Karls-Universität Heidelberg, Heidelberg; Germany.
[66(a)]Department of Physics, Chinese University of Hong Kong, Shatin, N.T., Hong Kong;[(b)]Department of Physics, University of Hong Kong, Hong Kong;[(c)]Department of Physics and Institute for Advanced Study, Hong Kong University of Science and Technology, Clear Water Bay, Kowloon, Hong Kong; China.
[67]Department of Physics, National Tsing Hua University, Hsinchu; Taiwan.
[68]IJCLab, Université Paris-Saclay, CNRS/IN2P3, 91405, Orsay; France.
[69]Centro Nacional de Microelectrónica (IMB-CNM-CSIC), Barcelona; Spain.
[70]Department of Physics, Indiana University, Bloomington IN; United States of America.
[71(a)]INFN Gruppo Collegato di Udine, Sezione di Trieste, Udine;[(b)]ICTP, Trieste;[(c)]Dipartimento Politecnico di Ingegneria e Architettura, Università di Udine, Udine; Italy.
[72(a)]INFN Sezione di Lecce;[(b)]Dipartimento di Matematica e Fisica, Università del Salento, Lecce; Italy.
[73(a)]INFN Sezione di Milano;[(b)]Dipartimento di Fisica, Università di Milano, Milano; Italy.
[74(a)]INFN Sezione di Napoli;[(b)]Dipartimento di Fisica, Università di Napoli, Napoli; Italy.
[75(a)]INFN Sezione di Pavia;[(b)]Dipartimento di Fisica, Università di Pavia, Pavia; Italy.
[76(a)]INFN Sezione di Pisa;[(b)]Dipartimento di Fisica E. Fermi, Università di Pisa, Pisa; Italy.
[77(a)]INFN Sezione di Roma;[(b)]Dipartimento di Fisica, Sapienza Università di Roma, Roma; Italy.
[78(a)]INFN Sezione di Roma Tor Vergata;[(b)]Dipartimento di Fisica, Università di Roma Tor Vergata, Roma; Italy.

[79(a)]INFN Sezione di Roma Tre;[(b)]Dipartimento di Matematica e Fisica, Università Roma Tre, Roma; Italy.
[80(a)]INFN-TIFPA;[(b)]Università degli Studi di Trento, Trento; Italy.
[81]Universität Innsbruck, Department of Astro and Particle Physics, Innsbruck; Austria.
[82]University of Iowa, Iowa City IA; United States of America.
[83]Department of Physics and Astronomy, Iowa State University, Ames IA; United States of America.
[84]Istinye University, Sariyer, Istanbul; Türkiye.
[85(a)]Departamento de Engenharia Elétrica, Universidade Federal de Juiz de Fora (UFJF), Juiz de Fora;[(b)]Universidade Federal do Rio De Janeiro COPPE/EE/IF, Rio de Janeiro;[(c)]Instituto de Física, Universidade de São Paulo, São Paulo;[(d)]Rio de Janeiro State University, Rio de Janeiro;[(e)]Federal University of Bahia, Bahia; Brazil.
[86]KEK, High Energy Accelerator Research Organization, Tsukuba; Japan.
[87]Graduate School of Science, Kobe University, Kobe; Japan.
[88(a)]AGH University of Krakow, Faculty of Physics and Applied Computer Science, Krakow;[(b)]Marian Smoluchowski Institute of Physics, Jagiellonian University, Krakow; Poland.
[89]Institute of Nuclear Physics Polish Academy of Sciences, Krakow; Poland.
[90]Faculty of Science, Kyoto University, Kyoto; Japan.
[91]Research Center for Advanced Particle Physics and Department of Physics, Kyushu University, Fukuoka ; Japan.
[92]L2IT, Université de Toulouse, CNRS/IN2P3, UPS, Toulouse; France.
[93]Instituto de Física La Plata, Universidad Nacional de La Plata and CONICET, La Plata; Argentina.
[94]Physics Department, Lancaster University, Lancaster; United Kingdom.
[95]Oliver Lodge Laboratory, University of Liverpool, Liverpool; United Kingdom.
[96]Department of Experimental Particle Physics, Jožef Stefan Institute and Department of Physics, University of Ljubljana, Ljubljana; Slovenia.
[97]School of Physics and Astronomy, Queen Mary University of London, London; United Kingdom.
[98]Department of Physics, Royal Holloway University of London, Egham; United Kingdom.
[99]Department of Physics and Astronomy, University College London, London; United Kingdom.
[100]Louisiana Tech University, Ruston LA; United States of America.
[101]Fysiska institutionen, Lunds universitet, Lund; Sweden.
[102]Departamento de Física Teorica C-15 and CIAFF, Universidad Autónoma de Madrid, Madrid; Spain.
[103]Institut für Physik, Universität Mainz, Mainz; Germany.
[104]School of Physics and Astronomy, University of Manchester, Manchester; United Kingdom.
[105]CPPM, Aix-Marseille Université, CNRS/IN2P3, Marseille; France.
[106]Department of Physics, University of Massachusetts, Amherst MA; United States of America.
[107]Department of Physics, McGill University, Montreal QC; Canada.
[108]School of Physics, University of Melbourne, Victoria; Australia.
[109]Department of Physics, University of Michigan, Ann Arbor MI; United States of America.
[110]Department of Physics and Astronomy, Michigan State University, East Lansing MI; United States of America.
[111]Group of Particle Physics, University of Montreal, Montreal QC; Canada.
[112]Fakultät für Physik, Ludwig-Maximilians-Universität München, München; Germany.
[113]Max-Planck-Institut für Physik (Werner-Heisenberg-Institut), München; Germany.
[114]Graduate School of Science and Kobayashi-Maskawa Institute, Nagoya University, Nagoya; Japan.
[115(a)]Department of Physics, Nanjing University, Nanjing;[(b)]School of Science, Shenzhen Campus of Sun Yat-sen University;[(c)]University of Chinese Academy of Science (UCAS), Beijing; China.
[116]Department of Physics and Astronomy, University of New Mexico, Albuquerque NM; United States of

America.
[117]Institute for Mathematics, Astrophysics and Particle Physics, Radboud University/Nikhef, Nijmegen; Netherlands.
[118]Nikhef National Institute for Subatomic Physics and University of Amsterdam, Amsterdam; Netherlands.
[119]Department of Physics, Northern Illinois University, DeKalb IL; United States of America.
[120](a)New York University Abu Dhabi, Abu Dhabi;(b)United Arab Emirates University, Al Ain; United Arab Emirates.
[121]Department of Physics, New York University, New York NY; United States of America.
[122]Ochanomizu University, Otsuka, Bunkyo-ku, Tokyo; Japan.
[123]Ohio State University, Columbus OH; United States of America.
[124]Homer L. Dodge Department of Physics and Astronomy, University of Oklahoma, Norman OK; United States of America.
[125]Department of Physics, Oklahoma State University, Stillwater OK; United States of America.
[126]Palacký University, Joint Laboratory of Optics, Olomouc; Czech Republic.
[127]Institute for Fundamental Science, University of Oregon, Eugene, OR; United States of America.
[128]Graduate School of Science, Osaka University, Osaka; Japan.
[129]Department of Physics, University of Oslo, Oslo; Norway.
[130]Department of Physics, Oxford University, Oxford; United Kingdom.
[131]LPNHE, Sorbonne Université, Université Paris Cité, CNRS/IN2P3, Paris; France.
[132]Department of Physics, University of Pennsylvania, Philadelphia PA; United States of America.
[133]Department of Physics and Astronomy, University of Pittsburgh, Pittsburgh PA; United States of America.
[134](a)Laboratório de Instrumentação e Física Experimental de Partículas - LIP, Lisboa;(b)Departamento de Física, Faculdade de Ciências, Universidade de Lisboa, Lisboa;(c)Departamento de Física, Universidade de Coimbra, Coimbra;(d)Centro de Física Nuclear da Universidade de Lisboa, Lisboa;(e)Departamento de Física, Universidade do Minho, Braga;(f)Departamento de Física Teórica y del Cosmos, Universidad de Granada, Granada (Spain);(g)Departamento de Física, Instituto Superior Técnico, Universidade de Lisboa, Lisboa; Portugal.
[135]Institute of Physics of the Czech Academy of Sciences, Prague; Czech Republic.
[136]Czech Technical University in Prague, Prague; Czech Republic.
[137]Charles University, Faculty of Mathematics and Physics, Prague; Czech Republic.
[138]Particle Physics Department, Rutherford Appleton Laboratory, Didcot; United Kingdom.
[139]IRFU, CEA, Université Paris-Saclay, Gif-sur-Yvette; France.
[140]Santa Cruz Institute for Particle Physics, University of California Santa Cruz, Santa Cruz CA; United States of America.
[141](a)Departamento de Física, Pontificia Universidad Católica de Chile, Santiago;(b)Millennium Institute for Subatomic physics at high energy frontier (SAPHIR), Santiago;(c)Instituto de Investigación Multidisciplinario en Ciencia y Tecnología, y Departamento de Física, Universidad de La Serena;(d)Universidad Andres Bello, Department of Physics, Santiago;(e)Instituto de Alta Investigación, Universidad de Tarapacá, Arica;(f)Departamento de Física, Universidad Técnica Federico Santa María, Valparaíso; Chile.
[142]Department of Physics, University of Washington, Seattle WA; United States of America.
[143]Department of Physics and Astronomy, University of Sheffield, Sheffield; United Kingdom.
[144]Department of Physics, Shinshu University, Nagano; Japan.
[145]Department Physik, Universität Siegen, Siegen; Germany.
[146]Department of Physics, Simon Fraser University, Burnaby BC; Canada.

[147]SLAC National Accelerator Laboratory, Stanford CA; United States of America.
[148]Department of Physics, Royal Institute of Technology, Stockholm; Sweden.
[149]Departments of Physics and Astronomy, Stony Brook University, Stony Brook NY; United States of America.
[150]Department of Physics and Astronomy, University of Sussex, Brighton; United Kingdom.
[151]School of Physics, University of Sydney, Sydney; Australia.
[152]Institute of Physics, Academia Sinica, Taipei; Taiwan.
[153](a)E. Andronikashvili Institute of Physics, Iv. Javakhishvili Tbilisi State University, Tbilisi;(b)High Energy Physics Institute, Tbilisi State University, Tbilisi;(c)University of Georgia, Tbilisi; Georgia.
[154]Department of Physics, Technion, Israel Institute of Technology, Haifa; Israel.
[155]Raymond and Beverly Sackler School of Physics and Astronomy, Tel Aviv University, Tel Aviv; Israel.
[156]Department of Physics, Aristotle University of Thessaloniki, Thessaloniki; Greece.
[157]International Center for Elementary Particle Physics and Department of Physics, University of Tokyo, Tokyo; Japan.
[158]Department of Physics, Tokyo Institute of Technology, Tokyo; Japan.
[159]Department of Physics, University of Toronto, Toronto ON; Canada.
[160](a)TRIUMF, Vancouver BC;(b)Department of Physics and Astronomy, York University, Toronto ON; Canada.
[161]Division of Physics and Tomonaga Center for the History of the Universe, Faculty of Pure and Applied Sciences, University of Tsukuba, Tsukuba; Japan.
[162]Department of Physics and Astronomy, Tufts University, Medford MA; United States of America.
[163]Department of Physics and Astronomy, University of California Irvine, Irvine CA; United States of America.
[164]University of West Attica, Athens; Greece.
[165]University of Sharjah, Sharjah; United Arab Emirates.
[166]Department of Physics and Astronomy, University of Uppsala, Uppsala; Sweden.
[167]Department of Physics, University of Illinois, Urbana IL; United States of America.
[168]Instituto de Física Corpuscular (IFIC), Centro Mixto Universidad de Valencia - CSIC, Valencia; Spain.
[169]Department of Physics, University of British Columbia, Vancouver BC; Canada.
[170]Department of Physics and Astronomy, University of Victoria, Victoria BC; Canada.
[171]Fakultät für Physik und Astronomie, Julius-Maximilians-Universität Würzburg, Würzburg; Germany.
[172]Department of Physics, University of Warwick, Coventry; United Kingdom.
[173]Waseda University, Tokyo; Japan.
[174]Department of Particle Physics and Astrophysics, Weizmann Institute of Science, Rehovot; Israel.
[175]Department of Physics, University of Wisconsin, Madison WI; United States of America.
[176]Fakultät für Mathematik und Naturwissenschaften, Fachgruppe Physik, Bergische Universität Wuppertal, Wuppertal; Germany.
[177]Department of Physics, Yale University, New Haven CT; United States of America.
[178]Yerevan Physics Institute, Yerevan; Armenia.
[a] Also Affiliated with an institute covered by a cooperation agreement with CERN.
[b] Also at An-Najah National University, Nablus; Palestine.
[c] Also at Borough of Manhattan Community College, City University of New York, New York NY; United States of America.
[d] Also at Center for Interdisciplinary Research and Innovation (CIRI-AUTH), Thessaloniki; Greece.
[e] Also at CERN, Geneva; Switzerland.
[f] Also at CMD-AC UNEC Research Center, Azerbaijan State University of Economics (UNEC); Azerbaijan.

[g] Also at Département de Physique Nucléaire et Corpusculaire, Université de Genève, Genève; Switzerland.
[h] Also at Departament de Fisica de la Universitat Autonoma de Barcelona, Barcelona; Spain.
[i] Also at Department of Financial and Management Engineering, University of the Aegean, Chios; Greece.
[j] Also at Department of Physics, California State University, Sacramento; United States of America.
[k] Also at Department of Physics, King's College London, London; United Kingdom.
[l] Also at Department of Physics, Stanford University, Stanford CA; United States of America.
[m] Also at Department of Physics, Stellenbosch University; South Africa.
[n] Also at Department of Physics, University of Fribourg, Fribourg; Switzerland.
[o] Also at Department of Physics, University of Thessaly; Greece.
[p] Also at Department of Physics, Westmont College, Santa Barbara; United States of America.
[q] Also at Faculty of Physics, Sofia University, 'St. Kliment Ohridski', Sofia; Bulgaria.
[r] Also at Hellenic Open University, Patras; Greece.
[s] Also at Imam Mohammad Ibn Saud Islamic University; Saudi Arabia.
[t] Also at Institucio Catalana de Recerca i Estudis Avancats, ICREA, Barcelona; Spain.
[u] Also at Institut für Experimentalphysik, Universität Hamburg, Hamburg; Germany.
[v] Also at Institute for Nuclear Research and Nuclear Energy (INRNE) of the Bulgarian Academy of Sciences, Sofia; Bulgaria.
[w] Also at Institute of Applied Physics, Mohammed VI Polytechnic University, Ben Guerir; Morocco.
[x] Also at Institute of Particle Physics (IPP); Canada.
[y] Also at Institute of Physics, Azerbaijan Academy of Sciences, Baku; Azerbaijan.
[z] Also at National Institute of Physics, University of the Philippines Diliman (Philippines); Philippines.
[aa] Also at Technical University of Munich, Munich; Germany.
[ab] Also at The Collaborative Innovation Center of Quantum Matter (CICQM), Beijing; China.
[ac] Also at TRIUMF, Vancouver BC; Canada.
[ad] Also at Università di Napoli Parthenope, Napoli; Italy.
[ae] Also at University of Colorado Boulder, Department of Physics, Colorado; United States of America.
[af] Also at Washington College, Chestertown, MD; United States of America.
[ag] Also at Yeditepe University, Physics Department, Istanbul; Türkiye.
[*] Deceased